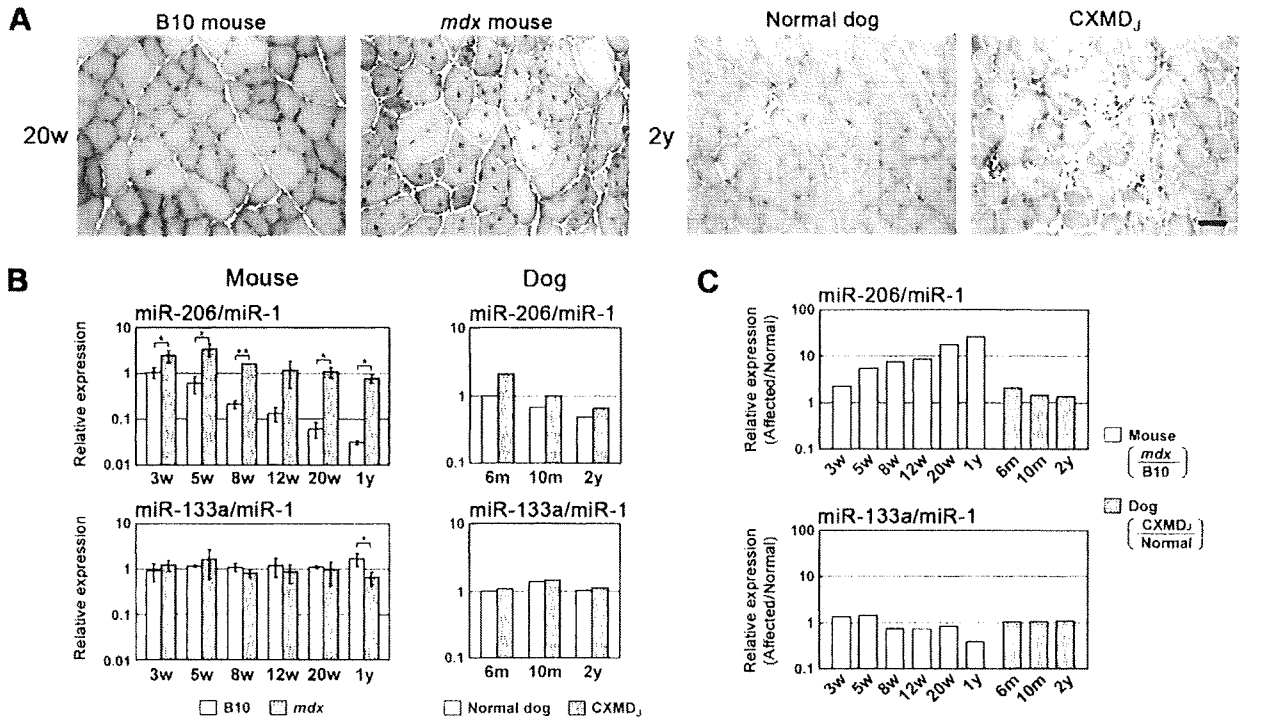

Fig. 3. **A**, Representative sections of B10, *mdx*, normal dog, and CXMD$_J$ TA muscles stained with hematoxylin and eosin. Note degenerating muscle fibers and inflammatory infiltrates in CXMD$_J$ muscle, in contrast to well-regenerated muscle fibers with central nuclei in *mdx* muscle. Bar, 50 μm. **B**, Expression levels of miR-206 and miR-133a are represented relative to that of miR-1, based on data shown in Fig. 1A and 2. Relative expression levels of miR-206 were elevated in *mdx* and CXMD$_J$ TA muscles as compared to respective control muscle. *, $P<0.05$; **, $P<0.01$. **C**, The relative expression of miR-206 or miR-133a to miR-1 in *mdx* and CXMD$_J$ TA muscles was compared to and represented relative to that in control TA muscles. Highly increased expression of miR-206 was observed in *mdx* muscles, as compared to CXMD$_J$ muscles .

is initiated within 3 days, new myotube formation is evident within 5 days, and muscle architecture is largely restored within 10 days (Hawke and Garry, 2001; see also Fig. 5B).

Consistent with previous studies (Kim *et al.*, 2006; Rao *et al.*, 2006), not only the expression of miR-206 but also those of miR-1 and miR-133a were markedly up-regulated during C2C12 differentiation (Fig. 4A). *In situ* hybridization analysis revealed that miR-206 was abundantly expressed in differentiated myotubes, in which intense signals for miR-206 were found in the sarcoplasm, especially in the perinuclear regions (Fig. 4B). Numerous mononucleated myoblasts, still found even in the differentiation medium, almost lacked miR-206 signals. For control experiments, hybridization with the omission of miR-206 probes or with the use of LacZ probes did not detect any specific and positive signals in C2C12 myoblasts or myotubes.

The CTX injection into TA muscles resulted in a decrease of ~100-fold in expression level of miR-206 on the first day post-injury and >100-fold decrease in those of miR-1 and miR-133a 3 days after CTX injection (Fig. 5A). The expression of miR-206 was induced on day 2 post-injury and increased markedly by 10-fold on day 5 post-injury. Its elevated expression level lasted until at least 4 week post-injury and was still significantly higher than the pre-operative level even 8 weeks after CTX injection. On the other hand, both miR-1 and miR-133a were similarly induced later on day 4 post-injury and their levels of expression increased gradually, returning close to the pre-operative levels by 4 weeks after CTX injection.

In situ hybridization analysis using miR-206 probes showed that newly formed myotubes or immature muscle fibers with centralized nuclei were intensely labeled with miR-206 probes in CTX-injured TA muscles (Fig. 5B). These results, together with the quantitative results described above, clearly indicated that miR-206 was highly expressed in regenerating muscle fibers. This is consistent with the present findings in dystrophic TA muscles of *mdx* mice.

Discussion

This study provided a detailed temporal analysis of muscle-specific miR-1, miR-133a, and miR-206 expression during

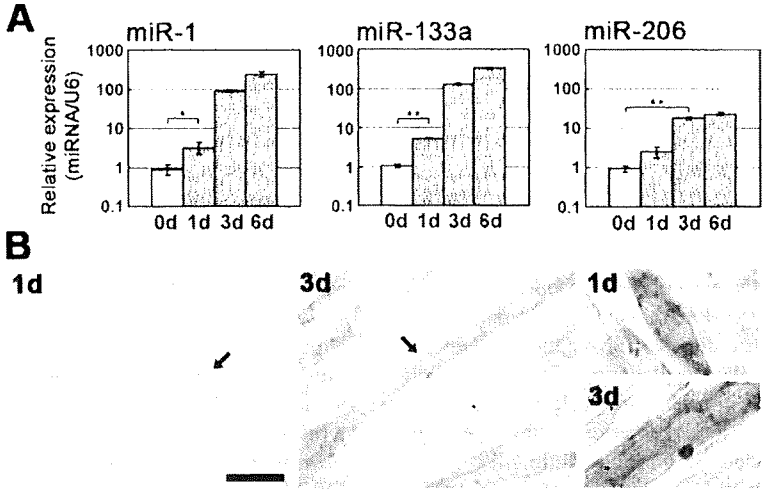

Fig. 4. **A**, Expression levels of miR-1, miR-133a, and miR-206 during C2C12 differentiation. C2C12 cells cultured in the differentiation medium for 0, 1, 3, or 6 days were used to determine expression levels of the three miRNAs by real-time RT-PCR. Results are presented as mean relative expression±SD; n=3. *, P<0.05; **, P<0.01. **B**, *In situ* hybridization analyses showed intense miR-206 signals in a newly formed myotube with two nuclei in day 1 cultures (1d) and large myotubes in day 3 cultures (3d). Pictures on the right side show enlarged views of the same myotubes indicated by arrows in the pictures on the left. Bar, 50 μm.

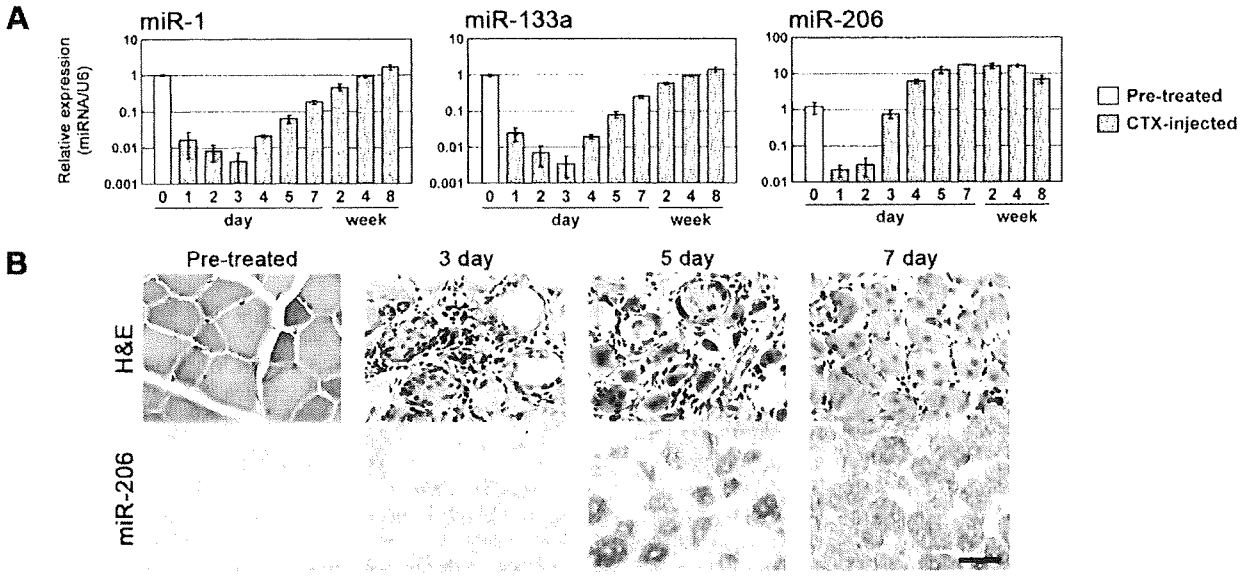

Fig. 5. **A**, Temporal expression profiles of miR-1, miR-133a, and miR-206 during the degeneration-regeneration process induced by CTX-injury. Using real-time RT-PCR, expression levels were determined in CTX-injected TA muscles at 0 day to 8 weeks post-injury. Results are presented as mean relative expression±SD; n=3. **B**, *In situ* hybridization analyses show intense miR-206 signals in regenerating fibers with central nuclei, but no signals in intact muscle fibers and many small cells, possibly inflammatory infiltrates and proliferating satellite cells. Bar, 50 μm.

the complete degeneration-regeneration process of mouse TA muscles injured by CTX. This quantitative analysis as well as the results of *in situ* hybridization analyses clearly indicated that miR-206 was highly expressed in myotubes newly formed from satellite cells. Similar increases in the expression of miR-206 in regenerating muscle fibers were found in *mdx* TA muscles, which have considerable regenerative capacity (Tanabe *et al.*, 1986; Coulton, *et al.*, 1988; Grounds and McGeachie *et al.*, 1992; Itagaki *et al.*, 1995). In contrast, CXMD$_J$ TA muscles, which exhibit much more

severe and more progressive degenerative alterations than those of *mdx* mice, expressed smaller amounts of miR-206 than controls.

miR-1, miR-133a, and miR-206 are transcribed during myogenesis and seem to be regulated by MyoD and myogenin (Rao *et al.*, 2006; Rosenberg *et al.*, 2006). miR-206 is transcribed independently of miR-1 and miR-133a, which are transcribed as a common pri-miRNA precursor from the miR-1/miR-133a locus, followed by alternative splicing to generate different primary transcripts (Rao *et al.*, 2006; Liu *et al.*, 2007). This is consistent with the present finding that miR-1 and miR-133a expression showed similar patterns in their induction and increase during CTX-induced regeneration. On the other hand, the onset of miR-206 expression temporally preceded those of miR-1 and miR-133a in CTX-induced regeneration. These observations suggested that miR-206 might be induced by MyoD, while miR-1 and miR-133a might be induced by myogenin, since the onset and temporal sequence of miR-206 and miR-1/miR-133a expression seem to coincide with those of MyoD and myogenin expression during myogenesis and CTX-induced regeneration (Megeney *et al.*, 1996; Yun and Wold, 1996; Launay *et al.*, 2001). After their induction by MyoD and myogenin, however, other factors must be involved in the expression of these miRNAs at later stages.

The early induction of miR-206 and its increased expression even after apparent recovery in CTX-induced regeneration emphasizes the suggestion that miR-206 may possess a variety of *in vivo* functions, such as myogenesis, synapse formation/elimination during reinnervation, maturation of muscle fibers, and maintenance of muscle integrity or contractility. Some functional roles of miR-206 during myogenesis, including myoblast fusion, have been proposed based on identification of its targets. miR-206 down-regulates DNA polymerase α, resulting in inhibition of DNA synthesis and withdrawal of myoblast proliferation, and thereby promoting muscle differentiation (Kim *et al.*, 2006). During myoblast fusion, connexin43 (Cx43), a component of gap junction channels, was down-regulated by miR-206 (Anderson *et al.*, 2006). During maturation of muscle fibers, utrophin is down-regulated and replaced at the sarcolemma by dystrophin. This suppression of utrophin has been shown to occur through miR-206 targeting to its 3'UTR (Rosenberg *et al.*, 2006). In addition, a search using TargetScan (www.targetscan.org/) predicted 480 potential targets for miR-206, including brain-derived neurotrophic factor (BDNF), nerve growth factor receptor (NGFR), insulin-like growth factor 1 (IGF-1), and insulin-like growth factor binding protein 5 (IGFBP5). These proteins may be involved in synapse formation/elimination during reinnervation and muscle mass regulation during muscle maturation, although it has yet to be verified whether their levels of expression are eventually down-regulated by miR-206.

Increased expression of miR-206 in *mdx* TA muscle may reflect active and efficient regeneration, whereas its decreased expression in CXMD$_J$ TA muscles may depict inactive and inefficient regeneration. In support of these suggestions, miR-206 introduction promotes C2C12 differentiation despite the presence of serum, whereas its inhibition by antisense oligonucleotide retards cell cycle withdrawal and differentiation (Kim *et al.*, 2006). As the expression of miR-206 is induced by MyoD and myogenin (Rao *et al.*, 2006; Rosenberg *et al.*, 2006), its decreased expression in CXMD$_J$ dystrophic muscles may suggest poor expression or instability of the myogenic factors. Their paucity and instability would affect satellite cell activation, myoblast differentiation into muscle fibers, and maturation of muscle fibers. MyoD mutant muscle was reported to be severely deficient in regenerative ability (Megeney *et al.*, 1996), whereas myogenin-deficient mice showed failure of myotube formation from myoblasts (Hasty *et al.*, 1993).

An additional point of interest is that the expression of miR-206 in control TA muscles is reduced with age, although newly formed muscle fibers show abundant expression. This fact implies that miR-206 functions in maintenance of muscle integrity and contractility may decline with age. To understand the multiple functions of miR-206 in not only myogenesis but also muscle maintenance, further studies, especially the identification of bona fide, biologically relevant targets for miR-206, will be required.

Acknowledgments. This work was supported in part by a Research Grant (17A-10, 20B-13) for Nervous and Mental Disorders from the Ministry of Health, Labor and Welfare, and by the High-Tech Research Center Project for Private Universities (MEXT. HAITEKU, 2004-2008).

References

Anderson, C., Catoe, H., and Werne, R. 2006. MIR-206 regulates connexin43 expression during skeletal muscle development. *Nucleic Acids Res.*, **34**: 5863–5871.

Boyd, S.D. 2008. Everything you wanted to know about small RNA but were afraid to ask. *Lab. Invest.*, **88**: 569–578.

Carè, A., Catalucci, D., Felicetti, F., Bonci, D., Addario, A., Gallo, P., Bang, M.L., Segnalini, P., Gu, Y., Dalton, N.D., Elia, L., Latronico, M.V., Høydal, M., Autore, C., Russo, M.A., Dorn, G.W. 2nd, Ellingsen, O., Ruiz-Lozano, P., Peterson, K.L., Croce, C.M., Peschle, C., and Condorelli, G. 2007. MicroRNA-133 controls cardiac hypertrophy. *Nat. Med.*, **13**: 613–618.

Chang, J., Nicolas, E., Marks, D., Sander, C., Lerro, A., Buendia, M.A., Xu, C., Mason, W.S., Moloshok, T., Bort, R., Zaret, K.S., and Taylor, J.M. 2004. miR-122, a mammalian liver-specific microRNA, is processed from hcr mRNA and may downregulate the high affinity cationic amino acid transporter CAT-1. *RNA Biol.*, **1**: 106–113.

Chen, J.F., Mandel, E.M., Thomson, J.M., Wu, Q., Callis, T.E., Hammond, S.M., Conlon, F.L., and Wang, D.Z. 2006. The role of microRNA-1 and microRNA-133 in skeletal muscle proliferation and differentiation. *Nat. Genet.*, **38**: 228–233.

Coulton, G.R., Curtin, N.A., Morgan, J.E., and Partridge, T.A. 1988. The *mdx* mouse skeletal muscle myopathy: II. Contractile properties. *Neuropathol. Appl. Neurobiol.*, **14**: 299–314.

Eisenberg, I., Eran, A., Nishino, I., Moggio, M., Lamperti, C., Amato, A.A., Lido,v H.G., Kang, P.B., North, K.N., Mitrani-Rosenbaum, S., Flanigan, K.M., Neely, L.A., Whitney, D., Beggs, A.H., Kohane, I.S.,

and Kunkel, L.M. 2007. Distinctive patterns of microRNA expression in primary muscular disorders. *Proc. Natl. Acad. Sci. USA*, **104**: 17016–17021.

Fazi, F., Rosa, A., Fatic, A., Gelmetti, V., De Marchis, M.L, Nervi, C., and Bozzoni, I. 2005. A minicircuitry comprised of microRNA-223 and transcription factors NFI-A and C/EBPalpha regulates human granulopoiesis. *Cell*, **123**: 819–831.

Grounds, M.D. and McGeachie, J.K. 1992. Skeletal muscle regeneration after crush injury in dystrophic *mdx* mice: an autoradiographic study. *Muscle Nerve*, **15**: 580–586.

Hasty, P., Bradley, A., Morris, J.H., Edmondson, D.G.., Venuti, J.M, Olson, E.N., and Klein, W.H. 1993. Muscle deficiency and neonatal death in mice with a targeted mutation in the myogenin gene. *Nature*, **364**: 501–506.

Hawke, T.J. and Garry, D.J. 2001. Myogenic satellite cells: physiology to molecular biology. *J. Appl. Physiol.*, **91**: 534–551.

Hornstein, E., Mansfield, J.H,, Yekta. S., Hu, J.K., Harfe, B.D., McManus, M.T., Baskerville, S., Bartel, D.P., and Tabin, C.J. 2005. The microRNA miR-196 acts upstream of Hoxb8 and Shh in limb development. *Nature*, **438**: 671–674.

Iorio, M.V., Ferracin, M., Liu, C.G., Veronese, A., Spizzo, R., Sabbioni, S., Magri, E., Pedriali, M., Fabbri, M., Campiglio, M., Ménard, S., Palazzo, J.P., Rosenberg, A., Musiani, P., Volinia, S., Nenci, I., Calin, G.A., Querzoli, P., Negrini, M., and Croce, C.M. 2005. MicroRNA gene expression deregulation in human breast cancer. *Cancer Res.*, **65**: 7065–7070.

Itagaki, Y., Saida, K., and Iwamura, K. 1995. Regenerative capacity of *mdx* mouse muscles after repeated applications of myo-necrotic bupivacaine. *Acta Neuropathol.*, **89**: 380–384.

Jopling, C.L., Yi, M., Lancaster, A.M., Lemon, S.M., and Sarnow, P. 2005. Modulation of hepatitis C virus RNA abundance by a liver-specific MicroRNA. *Science*, **309**: 1577–1581.

Kim, H.K., Lee, Y.S., Sivaprasad, U., Malhotra, A., and Dutta, A. 2006. Muscle-specific microRNA miR-206 promotes muscle differentiation. *J. Cell Biol.*, **174**: 677–687.

Kwon, C., Han, Z., Olson, E.N., and Srivastava, D. 2005. MicroRNA1 influences cardiac differentiation in Drosophila and regulates Notch signaling. *Proc. Natl. Acad. Sci. USA*, **102**: 18986–18991.

Lagos-Quintana, M., Rauhut, R., Yalcin, A., Meyer, J., Lendeckel, W., and Tuschl, T. 2002. Identification of tissue-specific microRNAs from mouse. *Curr. Biol.*, **12**: 735–739.

Launay, T., Armand, A.S., Charbonnier, F., Mira, J.C., Donsez, E., Gallien, C.L., and Chanoine, C. 2001. Expression and neural control of myogenic regulatory factor genes during regeneration of mouse soleus. *J. Histochem. Cytochem.*, **49**: 887–899.

Liu, N., Williams, A.H., Kim, Y., McAnally, J., Bezprozvannaya, S., Sutherland, L.B., Richardson, J.A., Bassel-Duby, R., and Olson, E.N. 2007. An intragenic MEF2-dependent enhancer directs muscle-specific expression of microRNAs 1 and 133. *Proc. Natl. Acad. Sci. USA*, **104**: 20844–20849.

Mansfield, J.H., Harfe, B.D., Nissen, R., Obenauer, J., Srineel, J., Chaudhuri, A., Farzan-Kashani, R., Zuker, M., Pasquinelli, A.E., Ruvkun, G., Sharp, P.A., Tabin, C.J., and McManus, M.T. 2004. MicroRNA-responsive 'sensor' transgenes uncover Hox-like and other developmentally regulated patterns of vertebrate microRNA expression. *Nat. Genet.*, **36**: 1079–1083.

McCarthy, J.J., Esser, K.A., and Andrade, F.H. 2007. MicroRNA-206 is overexpressed in the diaphragm but not the hindlimb muscle of *mdx* mouse. *Am. J. Physiol. Cell Physiol.*, **293**: C451–457.

Megeney, L.A., Kablar, B., Garrett, K., Anderson, J.E., and Rudnicki, M.A. 1996. MyoD is required for myogenic stem cell function in adult skeletal muscle. *Genes Dev.*, **10**: 1173–1183.

Rao, P.K., Kumar, R.M., Farkhondeh, M., Baskerville, S., and Lodish, H.F. 2006. Myogenic factors that regulate expression of muscle-specific microRNAs. *Proc. Natl. Acad. Sci. USA*, **103**: 8721–8726.

Rosenberg, M.I., Georges, S.A., Asawachaicharn, A., Analau, E., and Tapscott, S.J. 2006. MyoD inhibits Fstl1 and Utrn expression by inducing transcription of miR-206. *J. Cell Biol.*, **175**: 77–85.

Shimatsu, Y., Yoshimura, M., Yuasa, K., Urasawa, N., Tomohiro, M., Nakura, M., Tanigawa, M., Nakamura, A., and Takeda, S. 2005. Major clinical and histopathological characteristics of canine X-linked muscular dystrophy in Japan, CXMDJ. *Acta Myol.*, **24**: 145–154.

Sokol, N.S. and Ambros, V. 2005. Mesodermally expressed Drosophila microRNA-1 is regulated by Twist and is required in muscles during larval growth. *Genes Dev.*, **19**: 2343–2354.

Tanabe, Y., Esaki, K., and Nomura, T. 1986. Skeletal muscle pathology in X chromosome-linked muscular dystrophy (*mdx*) mouse. *Acta Neuropathol.*, **69**: 91–95.

van Rooij, E., Sutherland, L.B., Liu, N., Williams, A.H., McAnally, J., Gerard, R.D., Richardson, J.A., and Olson, E.N. 2006. A signature pattern of stress-responsive microRNAs that can evoke cardiac hypertrophy and heart failure. *Proc. Natl. Acad. Sci. USA*, **103**: 18255–18260.

van Rooij, E., Sutherland, L.B., Qi, X., Richardson, J.A., Hill, J., and Olson, E.N. 2007. Control of stress-dependent cardiac growth and gene expression by a microRNA. *Science*, **316**: 575–579.

Yang, B., Lin, H., Xiao, J., Lu, Y., Luo, X., Li, B., Zhang, Y., Xu, C., Bai, Y., Wang, H., Chen, G., and Wang, Z. 2007. The muscle-specific microRNA miR-1 regulates cardiac arrhythmogenic potential by targeting GJA1 and KCNJ2. *Nat. Med.*, **13**: 486–491.

Yun, K. and Wold, B. 1996. Skeletal muscle determination and differentiation: story of a core regulatory network and its context. *Curr. Opin. Cell Biol.*, **8**: 877–889.

Zhao, Y., Samal, E., and Srivastava, D. 2005. Serum response factor regulates a muscle-specific microRNA that targets Hand2 during cardiogenesis. *Nature*. **436**: 214–220.

Zhao, Y., Ransom, J.F., Li, A., Vedantham, V., von Drehle, M., Muth, A.N., Tsuchihashi, T., McManus, M.T., Schwartz, R.J., and Srivastava, D. 2007. Dysregulation of cardiogenesis, cardiac conduction, and cell cycle in mice lacking miRNA-1-2. *Cell*, **129**: 303–317.

(Received for publication, June 3, 2008, accepted, July 30, 2008 and published online, October 1, 2008)

The American Journal of Pathology, Vol. 173, No. 3, September 2008

DOI: 10.2353/ajpath.2008.070902

Musculoskeletal Pathology

Muscle CD31(−) CD45(−) Side Population Cells Promote Muscle Regeneration by Stimulating Proliferation and Migration of Myoblasts

Norio Motohashi,*† Akiyoshi Uezumi,* Erica Yada,* So-ichiro Fukada,* Kazuhiro Fukushima,*¶ Kazuhiko Imaizumi,† Yuko Miyagoe-Suzuki,* and Shin'ichi Takeda*

From the Department of Molecular Therapy, National Institute of Neuroscience, National Center of Neurology and Psychiatry, Tokyo; the Division for Therapies against Intractable Diseases,† Institute for Comprehensive Medical Science, Fujita Health University, Aichi; the Department of Immunology,‡ Graduate School of Pharmaceutical Sciences, Osaka University, Osaka; the Laboratory of Physiological Sciences,† Faculty of Human Sciences, Waseda University, Saitama; and the Third Department of Medicine, Neurology, and Rheumatology,¶ Shinshu University School of Medicine, Matsumoto, Japan*

CD31(−) CD45(−) side population (SP) cells are a minor SP subfraction that have mesenchymal stem cell-like properties in uninjured skeletal muscle but that can expand on muscle injury. To clarify the role of these SP cells in muscle regeneration, we injected green fluorescent protein (GFP)-positive myoblasts with or without CD31(−) CD45(−) SP cells into the tibialis anterior muscles of immunodeficient *NOD/scid* mice or dystrophin-deficient *mdx* mice. More GFP-positive fibers were formed after co-transplantation than after transplantation of GFP-positive myoblasts alone in both *mdx* and *NOD/scid* muscles. Moreover, grafted myoblasts were more widely distributed after co-transplantation than after transplantation of myoblasts alone. Immunohistochemistry with anti-phosphorylated histone H3 antibody revealed that CD31(−) CD45(−) SP cells stimulated cell division of co-grafted myoblasts. Genome-wide gene expression analyses showed that these SP cells specifically express a variety of extracellular matrix proteins, membrane proteins, and cytokines. We also found that they express high levels of matrix metalloproteinase-2 mRNA and gelatinase activity. Furthermore, matrix metalloproteinase-2 derived from CD31(−) CD45(−) SP cells promoted migration of myoblasts *in vivo*. Our results suggest that CD31(−) CD45(−) SP cells support muscle regeneration by promoting proliferation and migration of myoblasts. Future studies to further define the molecular and cellular mechanisms of muscle regeneration will aid in the development of cell therapies for muscular dystrophy. ***(Am J Pathol 2008, 173:781–791; DOI: 10.2353/ajpath.2008.070902)***

Regeneration of skeletal muscle is a complex but well-organized process involving activation, proliferation, and differentiation of myogenic precursor cells, infiltration of macrophages to remove necrotic tissues, and remodeling of the extracellular matrix.[1–3] Muscle satellite cells are myogenic precursor cells that are located between the basal lamina and the sarcolemma of myofibers in a quiescent state, and are primarily responsible for muscle fiber regeneration in adult muscle.[4] Recent studies also demonstrated that a fraction of satellite cells self-renew and behave as muscle stem cells *in vivo*.[5,6] On the other hand, several research groups reported multipotent stem cells derived from skeletal muscle. These include muscle-derived stem cells,[7] multipotent adult precursor cells,[8] myogenic-endothelial progenitors,[9] CD34(+) Sca-1(+) cells,[10] CD45(+) Sca-1 (+) cells,[11] mesoangioblasts,[12] and pericytes,[13] and all were demonstrated to contribute to muscle regeneration as myogenic progenitor cells.

Side population (SP) cells are defined as the cell fraction that efficiently effluxes Hoechst 33342 dye and therefore shows a unique pattern on fluorescence-activated cell sorting (FACS) analysis.[14] Muscle SP cells are proposed to be multipotent[15,16] and are clearly distinguished from satellite

Supported by the Ministry of Health, Labor, and Welfare (grant 16b-2 for research on nervous and mental disorders, health science research grant h16-genome-003 for research on the human genome and gene therapy, grants h15-kokoro-021, H18-kokoro-019 for research on brain science); the Ministry of Education, Culture, Sports, Science, and Technology (grants-in-aid for scientific research 16590333 and 18590392); and the Japan Space Forum (ground-based research program for space utilization).

Accepted for publication June 4, 2008.

Supplemental material for this article can be found on *http://ajp.amjpathol.org*.

Address reprint requests to Yuko Miyagoe-Suzuki, M.D., Ph.D., Department of Molecular Therapy, National Institute of Neuroscience, National Center of Neurology and Psychiatry, 4-1-1 Ogawa-higashi, Kodaira, Tokyo 187-8502, Japan. E-mail: miyagoe@ncnp.go.jp.

cells.[17] Previous reports showed that muscle SP cells participated in regeneration of dystrophic myofibers after systemic delivery[15] and gave rise to muscle satellite cells after intramuscular injection into cardiotoxin (CTX)-treated muscle.[17] Muscle SP cells adapted to myogenic characteristics after co-culture with proliferating satellite cells/myoblasts *in vitro*,[17] and expressed a satellite cell-specific transcription factor, Pax7, after intra-arterial transplantation.[18] However, the extent to which muscle SP cells participate in muscle fiber regeneration as myogenic progenitor cells is still primarily unknown. Importantly, Frank and colleagues[19] recently showed that muscle SP cells secret BMP4 and regulate proliferation of BMP receptor1α (+) Myf5^{high} myogenic cells in human fetal skeletal muscle, raising the possibility that SP cells in adult muscle play regulatory roles during muscle regeneration.

Previously we showed that skeletal muscle-derived SP cell fraction are heterogeneous and contain at least three subpopulations: CD31(+) CD45(−) SP cells, CD31(−) CD45(+) SP cells, and CD31(−) CD45(−) SP cells.[20] These three SP subpopulations have distinct origins, gene expression profiles, and differentiation potentials.[20] CD31(+) CD45(−) SP cells account for more than 90% of all SP cells in normal skeletal muscle, take up Ac-LDL, and are associated with the vascular endothelium. CD31(+) CD45(−) SP cells did not proliferate after CTX-induced muscle injury. Bone marrow transplantation experiments demonstrated that CD31(−) CD45(+) SP cells are recruited from bone marrow into injured muscle. A few of them are thought to participate in fiber formation.[21] Cells of the third SP subfraction, CD31(−) CD45(−), constitute only 5 to 6% of all SP cells in adult normal skeletal muscle, but they actively expand in the early stages of muscle regeneration and return to normal levels when muscle regeneration is completed. Although CD31(−) CD45(−) SP cells are the only SP subset that exhibited the capacity to differentiate into myogenic, adipogenic, and osteogenic cells *in vitro*,[20] their myogenic potential *in vivo* is limited compared with satellite cells. Therefore, we hypothesized that CD31(−) CD45(−) SP cells might play critical roles during muscle regeneration other than as myogenic stem cells.

In the present study, we demonstrate that the efficacy of myoblast transfer is markedly improved by co-transplantation of CD31(−) CD45(−) SP cells in both regenerating immunodeficient *NOD/scid* and dystrophin-deficient *mdx* mice. We also show that CD31(−) CD45(−) SP cells increased the proliferation and migration of grafted myoblasts *in vivo* and *in vitro*. We further show that CD31(−) CD45(−) SP cell-derived matrix metalloproteinase (MMP)-2 greatly promotes the migration of myoblasts *in vivo*. Our findings would provide us insights into the molecular and cellular mechanisms of muscle regeneration, and also help us develop cell therapy for muscular dystrophy.

Materials and Methods

Animals

All experimental procedures were approved by the Experimental Animal Care and Use Committee at the National Institute of Neuroscience. Eight- to twelve-week-old C57BL/6 mice and *NOD/scid* mice were purchased from Nihon CLEA (Tokyo, Japan). MMP-2-null mice were obtained from Riken BioResource Center (Tsukuba, Japan).[22] GFP-transgenic mice (GFP-Tg) were kindly provided by Dr. M. Okabe (Osaka University, Osaka, Japan). C57BL/6-background *mdx* mice were generously given by Dr. T. Sasaoka (National Institute for Basic Biology, Aichi, Japan) and maintained in our animal facility.

Isolation of Muscle SP Cells

To evoke muscle regeneration, CTX (10 μmol/L in saline; Sigma, St. Louis, MO) was injected into the tibialis anterior (TA) (50 μl), gastrocnemius (150 μl), and quadriceps femoris muscles (100 μl) of 8- to 12-week-old GFP-Tg mice, C57BL/6 mice, MMP-2-null mice, and their wild-type littermates; 3 days later, SP cells were isolated from the muscles as described by Uezumi and colleagues.[20] In brief, limb muscles were digested with 0.2% type II collagenase (Worthington Biochemical, Lakewood, NJ) for 90 minutes at 37°C. After elimination of erythrocytes by treatment with 0.8% NH_4Cl in Tris-buffer (pH 7.15), mononucleated cells were suspended at 10^6 cells per ml in Dulbecco's modified Eagle's medium (Wako, Richmond, VA) containing 2% fetal bovine serum (JRH Biosciences, Inc., Kansas City, KS), 10 mmol/L Hepes, and 5 μg/ml Hoechst 33342 (Sigma), incubated for 90 minutes at 37°C in the presence or the absence of 50 μmol/L Verapamil (Sigma), and then incubated with phycoerythrin (PE)-conjugated anti-CD31 antibody (1:200, clone 390; Southern Biotechnology, Birmingham, AL) and PE-conjugated anti-CD45 (1:200, clone 30-F11; BD Pharmingen, Franklin Lakes, NJ) for 30 minutes on ice. Dead cells were eliminated by propidium iodide staining. Analysis and cell sorting were performed on an FACS VantageSE flow cytometer (BD Bioscience, Franklin Lakes, NJ). APC-conjugated anti-CD90, Sca-1, CD34, CD49b, CD14, CD124, c-kit, CD14 (BD Pharmingen), CD44 (Southern Biotechnology Associates), and CD133 (eBioscience, San Diego, CA) were used at 1:200 dilution.

Preparation of Satellite Cell-Derived Myoblasts and Macrophages

Satellite cells were isolated from GFP-Tg mice or C57BL/6 mice by using SM/C-2.6 monoclonal antibody[23] and expanded *in vitro* in Dulbecco's modified Eagle's medium containing 20% fetal bovine serum and 2.5 ng/ml of basic fibroblast growth factor (Invitrogen, Carlsbad, CA) for 4 days before transplantation. Macrophages were isolated from C57BL/6 mice 3 days after CTX injection. Mononucleated cells were stained with anti-Mac-1-PE (1:200, clone M1/70; BD PharMingen) and anti-F4/80-APC (1:200, clone Cl. A3-1; Serotec, Oxford, UK). Mac-1(+) F4/80(+) cells were isolated by cell sorting as macrophages.

Cell Transplantation

To induce muscle regeneration, 100 μl of 10 μmol/L CTX was injected into the TA muscle of *NOD/scid* muscles,

and 24 hours later, 30 μl of cell suspensions containing 3×10^4 myoblasts, 3×10^4 CD31(−) CD45(−) SP cells, or 3×10^4 GFP(+) myoblasts plus 2×10^4 CD31(−) CD45(−) SP cells were directly injected into the TA muscles of 8-week-old *NOD/scid* or *mdx* mice. At several time points after transplantation, the muscles were dissected, fixed in 4% paraformaldehyde for 30 minutes, immersed in 10% sucrose/phosphate-buffered saline (PBS) and then in 20% sucrose/PBS, and frozen in isopentane cooled with liquid nitrogen.

Retrovirus Transduction in Vitro

Red fluorescent protein (DsRed) cDNA (BD Biosciences, San Diego, CA) was cloned into a retrovirus plasmid, pMXs, kindly provided by Dr. T. Kitamura of the University of Tokyo, Tokyo, Japan.[24] Viral particles were prepared by introducing the resultant pMXs-DsRed into PLAT-E retrovirus packaging cells,[25] and the filtered supernatant was added to the myoblast culture. The next day, DsRed(+) myoblasts were collected by flow cytometry.

Immunohistochemistry

We cut the entire TA muscle tissues on a cryostat into 6-μm cross sections, and observed all serial sections under fluorescence microscopy. We then selected two or three sections in which GFP(+) cells were found most frequently. The sections were then blocked with 5% goat serum (Cedarlane, Hornby, Canada) in PBS for 15 minutes, and then reacted with anti-GFP antibody (Chemicon International, Temecula, CA), anti-laminin α2 antibody (4H8-2; Alexis, San Diego, CA), anti-phospho-histone H3 antibody (Upstate Biotechnology, Lake Placid, NY), or anti-DsRed antibody (Clontech, Palo Alto, CA) at 4°C overnight. Dystrophin was detected using a monoclonal antibody, Dys-2 (Novocastra, Newcastle on Tyne, UK), and a M.O.M. Kit (Vector Laboratories, Burlingame, CA). The sections were then incubated with appropriate combinations of Alexa 488-, 568-, or 594-labeled secondary antibodies (Molecular Probes, Eugene, OR) and TOTO-3 (Molecular Probes), and photographed using a confocal laser-scanning microscope system TCSSP (Leica, Heidelberg, Germany). The area occupied by GFP(+) cells or myofibers was measured by using Image J software (National Institutes of Health, Bethesda, MD) on cross sections from three independent experiments, and defined as the distribution area.

RNA Isolation and Real-Time Polymerase Chain Reaction (PCR)

Total RNA was isolated from muscles using TRIzol (Invitrogen). First strand cDNA was synthesized using a QuantiTect reverse transcription kit (Qiagen, Hilden, Germany). The levels of GFP mRNA and 18S rRNA were quantified using SYBR Premix Ex Taq (Takara, Otsu, Shiga, Japan) on a MyiQ single-color system (Bio-Rad Laboratories, Richmond, CA) following the manufacturer's instructions. Primer sequences for real-time PCR were: 18s rRNA, forward: 5′-TACCCTGGCGGTGGGATTAAC-3′, reverse: 5′-CGAGAGAAGACCACGCCAAC-3′ and EGFP, forward: 5′-GACGTAAACGGCCACAAGTT-3′, reverse: 5′-AAGTCGTGCTGCTTCATGTG-3′. The expression levels of *MMP-2* and *MMP-9* were evaluated by conventional reverse transcriptase (RT)-PCR using the following primers: MMP-2, forward: 5′-TGCAAGGCAGTGGTCATAGCT-3′, reverse: 5′-AGCCAGTCGGATTTGATGCT-3′.

Cell Proliferation Assay

CD31(−) CD45(−) SP cells or 10T1/2 cells were cultured in Dulbecco's modified Eagle's medium containing 20% fetal bovine serum for 5 days, and the supernatants were collected as conditioned medium. Myoblasts were plated on 96-well culture plates at a density of 5000 cells/well and cultured in conditioned medium for 3 days. BrdU was then added to the culture medium (final concentration, 10 μmol/L). Twenty-four hours later, BrdU uptake was quantified by a cell proliferation enzyme-linked immunosorbent assay, a BrdU kit (Roche Diagnostics, Meylan, France), and Lumi-Image F1 (Roche).

Gene Expression Profiling

Total RNAs were extracted from CD31(−) CD45(−) SP cells, macrophages, or myoblasts using an RNeasy RNA isolation kit (Qiagen). cDNA synthesis, biotin-labeled target synthesis, MOE430A GeneChip (Affymetrix, Santa Clara, CA) array hybridization, staining, and scanning were performed according to standard protocols supplied by Affymetrix. The quality of the data presented in this study was controlled by using the Microarray Suite MAS 5.0 (Affymetrix). The MAS-generated raw data were uploaded to GeneSpring software version 7.0 (Silicon Genetics, Redwood City, CA). The software calculates signal intensities, and each signal was normalized to a median of its values in all samples or the 50th percentile of all signals in a specific hybridization experiment. Fold ratios were obtained by comparing normalized data of CD31(−) CD45(−) SP cells and macrophages or myoblasts.

In Situ *Zymography*

CD31(−) CD45(−) SP cells, myoblasts, and macrophages were isolated from regenerating muscles 3 days after CTX injection by cell sorting and collected by a Cytospin3 centrifuge (ThermoShandon, Cheshire, UK) on DQ-gelatin-coated slides (Molecular Probes). The slides were then incubated for 24 hours at 37°C in the presence or absence of GM6001 (a broad-spectrum inhibitor of MMPs, 50 μmol/L; Calbiochem, San Diego, CA) or E-64 (a cysteine protease inhibitor, 50 mmol/L; Calbiochem). Fluorescence of fluorescein isothiocyanate was detected with excitation at 460 to 500 nm and emission at 512 to 542 nm.

Statistics

Statistical differences were determined by Student's unpaired *t*-test. For comparison of more than two groups,

one-way analysis of variance was used. All values are expressed as means ± SE. A probability of less than 5% ($P < 0.05$) or 1% ($P < 0.01$) was considered statistically significant.

Results

Marker Expression on Muscle-Derived CD31(−) CD45(−) SP Cells

When incubated with 5 μg/ml of Hoechst 33342 dye at 37°C for 90 minutes, 1 to 3% of muscle mononuclear cells show the SP phenotype (Figure 1A). Previously, we reported that muscle SP cells can be further divided into three subpopulation, CD31(−) CD45(−) cells, CD31(−) CD45(+) cells, and CD31(+) CD45(−) SP cells (Figure 1B).[20] The CD31(−) CD45(−) SP cells did not express Pax3, Pax7, or Myf5, indicating that they are not yet committed to the muscle lineage.[20] RT-PCR suggested that CD31(−) CD45(−) SP cells have mesenchymal cell characteristics.[20] To further clarify the properties of CD31(−) CD45(−) SP cells, we analyzed their cell surface markers. CD31(−) CD45(−) SP cells were negative for CD124, CD133, CD14, c-kit (Figure 1B), and CD184 (data not shown), weakly positive for CD34 and CD49b, and strongly positive for Sca-1, CD44, and CD90 (Figure 1). The FACS patterns shown in Figure 1B suggested that CD31(−) CD45(−) SP cells are a homogeneous cell population. CD14 is an exception. A small fraction of CD31(−) CD45(−) SP cells were strongly positive for CD14, but the majority weakly expressed this marker. The function of CD14^{high} CD31(−) CD45(−) SP cells remains to be determined.

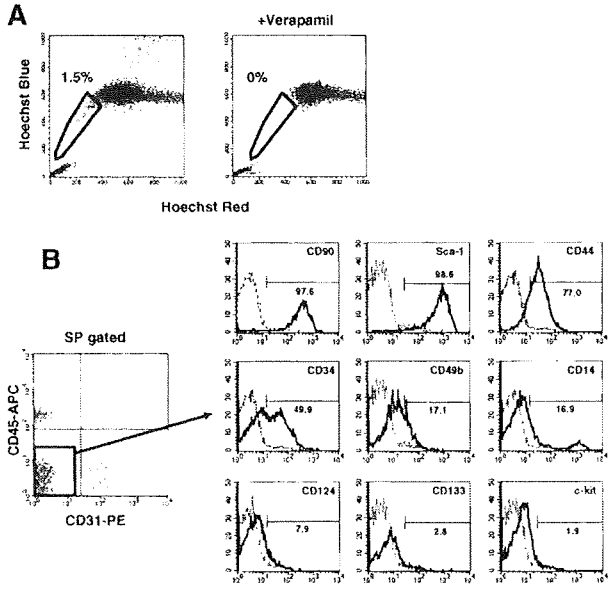

Figure 1. Cell surface markers on CD31(−) CD45(−) SP cells from regenerating muscle. **A:** Mononuclear cells were prepared from limb muscles of C57BL/6 mice at 3 days after CTX injection, incubated with 5 μmol/L Hoechst 33342 with (**right**) or without (**left**) Verapamil, and analyzed by a cell sorter. SP cells are shown by polygons. The numbers indicate the percentage of SP cells in all mononuclear cells. **B: Left:** Expression of CD45 and CD31 on muscle SP cells. **Right:** The expression of surface markers (CD90, Sca-1, CD44, CD34, CD49b, CD14, CD124, CD133, and c-kit) on CD31(−) CD45(−) SP cells was further analyzed by FACS. The *x* axis shows the fluorescence intensity, and the *y* axis indicates cell numbers. Solid lines are with antibodies; dotted lines are negative controls.

Efficiency of Myoblast Transplantation Is Increased by Co-Transplantation of Muscle CD31(−) CD45(−) SP Cells in NOD/scid Mice

To clarify the functions of CD31(−) CD45(−) SP cells during muscle regeneration, we isolated myoblasts from GFP-transgenic mice (GFP-Tg) and injected them (3×10^4 cells/muscle) with or without CD31(−) CD45(−) SP cells (2×10^4 cells/muscle) into TA muscles of immunodeficient *NOD/scid* mice (Figure 2A). CTX was injected into recipient muscles 24 hours before cell transplantation to induce muscle regeneration. Two weeks after transplantation, the contribution of grafted myoblasts to muscle regeneration was investigated by immunodetection of GFP(+) myofibers. Co-transplantation of GFP(+) myoblasts with nonlabeled CD31(−) CD45(−) SP cells produced a higher number of GFP(+) myofibers than transplantation of GFP(+) myoblasts alone (Figure 2, B and C). Furthermore, the average diameter of GFP(+) myofibers was significantly larger in co-transplanted muscles than in muscles transplanted with myoblasts alone (Figure 2D). These results suggest that more myoblasts participated in myofiber formation after co-transplantation than after single transplantation, injected SP cells promoted growth of regenerating myofibers, or both.

Co-transplantation of Myoblasts with Muscle CD31(−) CD45(−) SP Cells Significantly Increased Efficiency of Myoblast Transplantation in mdx Mice

Next, co-transplantation experiments were performed using 8-week-old dystrophin-deficient *mdx* mice as a host. Three kinds of transplantations were performed: 3×10^4 myoblasts derived from GFP-Tg mice, 3×10^4 CD31(−) CD45(−) SP cells derived from GFP-Tg mice, or a mixture of GFP(+) 3×10^4 myoblasts and 2×10^4 CD31(−) CD45(−) SP cells derived from C57BL/6 mice (Figure 3A).

When analyzed at 2 weeks after transplantation, a much higher number of GFP(+) myofibers were detected on cross-sections after co-transplantation of myoblasts and CD31(−) CD45(−) SP cells than after transplantation of GFP(+) myoblasts alone (Figure 3, B and C). On the other hand, transplantation of GFP(+) SP cells alone resulted in formation of few GFP(+) myofibers. This observation is consistent with our previous report.[20] Co-transplantation of myoblasts and CD31(−) CD45(−) SP cells also gave rise to more myofibers expressing dystrophin at the sarcolemma in dystrophin-deficient *mdx* muscles than transplantation of myoblasts alone (data not shown). Again, the diameter of GFP(+) myofibers was significantly larger in co-transplanted muscles than in muscles transplanted with myoblasts or CD31(−) CD45(−) SP cells alone (Figure 3D).

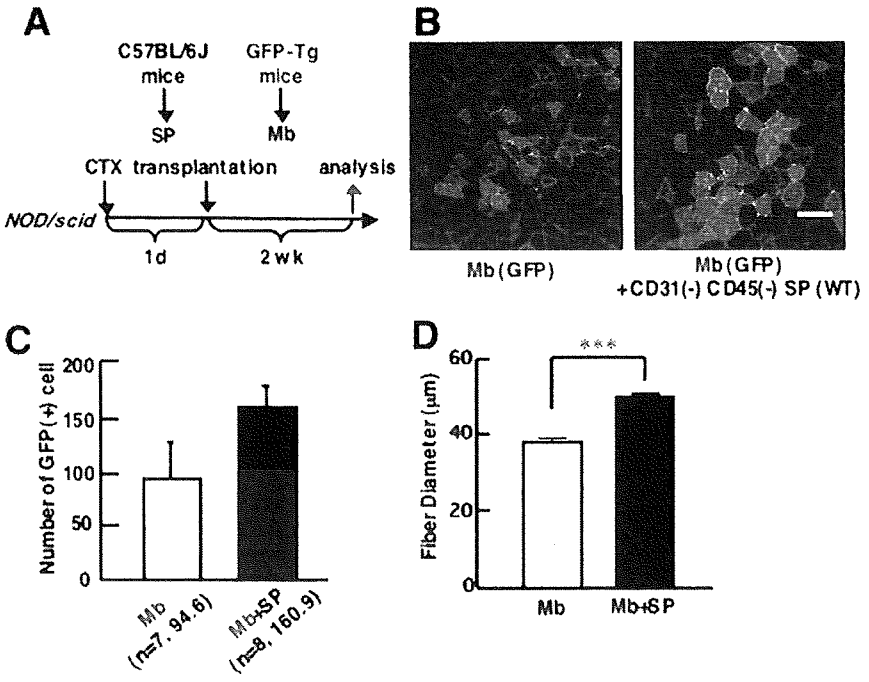

Figure 2. Co-transplantation of myoblasts and CD31(−) CD45(−) SP cells into skeletal muscle of immunodeficient *NOD/scid* mice promotes myofiber formation by transplanted myoblasts. **A:** Schematic protocol of co-transplantation experiments. CTX was injected into TA muscle 1 day before transplantation. Then, GFP(+) myoblasts (Mb) alone or with a mixture of GFP(+) myoblasts and CD31(−) CD45(−) SP cells derived from wild-type (WT) mice were transplanted to CTX-injected TA muscles of 8- to 12-week-old *NOD/scid* mice, and sampled 2 weeks after transplantation. **B:** Cross-sections of transplanted TA muscles stained with anti-GFP (green) and anti-laminin-α2 chain (red) antibodies. Nuclei were stained with TOTO3 (blue). **C:** The number of GFP(+) fibers per cross section of transplanted TA muscle. Values are means with SE (seven to eight mice in each group). $^{**}P < 0.01$. **D:** Average diameters of GFP(+) fibers in the TA muscles transplanted with myoblasts (Mb) or myoblasts plus CD31(−) CD45(−) SP cells (Mb + SP). Values are means with SE. $^{***}P < 0.001$. Scale bar = 80 μm.

The transplantation efficiency of myoblasts in *mdx* mice was 40 to 60% lower than that in *NOD/scid* mice. In the present study, *mdx* mice were not treated with any immunosuppressant. Although cellular infiltration was not evident when examined 2 weeks after transplantation (data not shown), some immune reaction might be evoked and eliminate myoblasts transplanted into *mdx* muscle.

Localization of Transplanted Myoblasts and CD31(−) CD45(−) SP Cells after Intramuscular Injection

To examine the interaction between grafted myoblasts and CD31(−) CD45(−) SP cells during muscle regeneration, we labeled C57BL/6 myoblasts with a retrovirus vector expressing a red fluorescent protein, DsRed. CD31(−) CD45(−) SP cells were isolated from GFP-Tg mice. We then injected a mixture of DsRed(+) myoblasts and GFP(+) CD31(−) CD45(−) SP cells into CTX-injected *NOD/scid* TA muscles. At 24 hours after transplantation, DsRed(+) myoblasts and GFP(+) CD31(−) CD45(−) SP cells were observed clearly (Figure 4A). At 48 hours after transplantation, immunohistochemistry revealed that grafted CD31(−) CD45(−) SP cells expanded, and surrounded both grafted myoblasts and damaged myofibers, but rarely fused with myoblasts (Figure 4B).

CD31(−) CD45(−) SP Cells Promote Proliferation of Myoblasts in Vivo *and* in Vitro

Next, to clarify the mechanism by which co-transplanted CD31(−) CD45(−) SP cells increased the contribution of grafted myoblasts to myofiber regeneration, we investigated the survival of grafted myoblasts after transplantation (Figure 5). GFP(+) myoblasts were injected into TA muscles of *NOD/scid* mice with or without unlabeled CD31(−) CD45(−) SP cells. At 24, 48, and 72 hours after transplantation, injected TA muscles were dissected, and the GFP mRNA level in injected muscles was evaluated by using real-time PCR (Figure 5A). There was a decline of the GFP mRNA level of injected muscles from 24 to 72 hours after injection (Figure 5B) with no differences in survival rates between single transplantation and co-transplantation.

At 48 and 72 hours after transplantation, however, GFP mRNA levels were slightly higher in co-injected muscle than in muscle injected with myoblasts alone (Figure 5B). Therefore, we directly counted the number of GFP(+) myoblasts at 72 hours after transplantation. As shown in Figure 6, A and B, many more GFP(+) myoblasts were detected in co-transplanted muscles than in myoblast-transplanted muscles (Figure 6, A and B). In addition, GFP(+) cells were more widely spread in the co-injected muscles than in muscles transplanted with myoblasts alone (Figure 6C).

To determine whether CD31(−) CD45(−) SP cells promote proliferation of implanted myoblasts, we dissected the muscles at 48 hours after transplantation, and stained the cross-sections with anti-phosphorylated histone H3 antibody, a marker of the mitotic phase of the cell cycle. Co-transplantation of myoblasts with CD31(−) CD45(−) SP cells significantly increased the percentage of mitotic GFP(+) cells compared with transplantation of myoblasts alone (Figure 6D). These observations suggest that co-injection of CD31(−) CD45(−) SP cells promoted proliferation of grafted myoblasts.

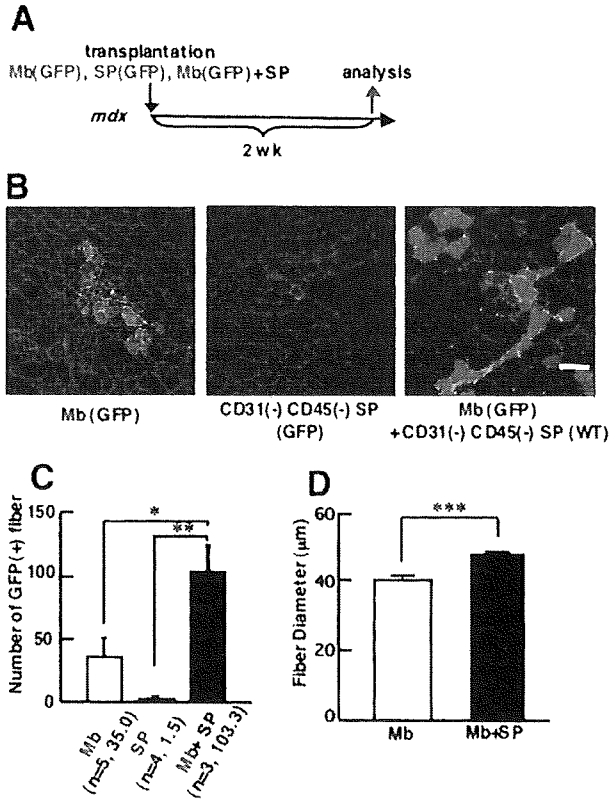

Figure 3. Co-transplantation of CD31(−) CD45(−) SP cells and myoblasts improves efficiency of myoblast transfer in dystrophin-deficient *mdx* mice. **A:** Schematic protocol of experiments. GFP(+) myoblasts alone (3×10^4), GFP(+) CD31(−) CD45(−) SP cells alone (3×10^4 cells), or a mixture of GFP(+) myoblasts (3×10^4) and CD31(−) CD45(−) SP cells (2×10^4) were directly injected into TA muscles of 8-week-old *mdx* mice, and the muscles were sampled 2 weeks after transplantation. **B:** Cross-sections of transplanted TA muscles stained with anti-GFP (green) and anti-laminin-α2 chain (red) antibodies. Nuclei were stained with TOTO3 (blue). **C:** The number of GFP(+) fibers per cross section. Myoblasts gave rise to more myofibers when co-transplanted with CD31(−) CD45(−) SP cells (Mb + SP) than when transplanted alone (Mb). Transplantation of only GFP(+) SP cells resulted in formation of few myofibers (SP). Values are means with SE ($n = 3$ to 5 mice). $^*P < 0.05$, $^{**}P < 0.01$. **D:** Average diameters of GFP(+) fibers in the TA muscles transplanted with myoblasts (Mb) or with myoblasts plus CD31(−) CD45(−) SP cells (Mb + SP). Values are means with SE. $^{***}P < 0.001$. Scale bar = 80 μm.

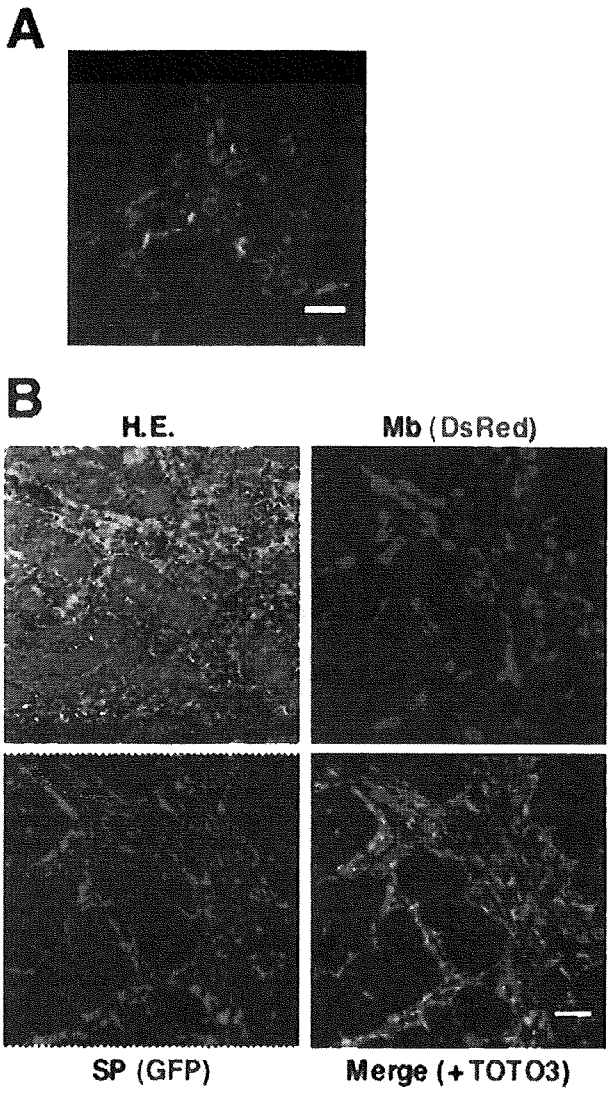

Figure 4. Behavior of GFP$^+$ CD31(−) CD45(−) SP cells and DsRed-labeled myoblasts after transplantation. **A:** *NOD/scid* TA muscles were injected with CTX 24 hours before transplantation. Then, myoblasts transduced with a retrovirus vector expressing DsRed were injected together with GFP(+) CD31(−) CD45(−) SP cells into the muscles. The muscles were dissected 24 hours after the transplantation, sectioned, and stained with anti-DsRed (red) and anti-GFP antibodies (green). Nuclei were stained with TOTO3 (blue). **B:** Representative image of DsRed(+) myoblasts and GFP(+) SP cells 48 hours after co-transplantation. One serial section was stained with H&E. Scale bars = 40 μm.

Next, to examine whether CD31(−) CD45(−) SP cells directly promote proliferation of myoblasts or not, we performed an *in vitro* proliferation assay using primary myoblasts and conditioned medium (CM) of CD31(−) CD45(−) SP cells and CM of 10T1/2 cells. BrdU uptake analysis showed that SP-CM more strongly stimulated the proliferation of myoblasts than 10T1/2-CM did (Figure 6E). The results suggest that CD31(−) CD45(−) SP cells promote proliferation of injected myoblasts at least in part by producing soluble factors.

Gene Expression Profiling of CD31(−) CD45(−) SP Cells

To identify the growth factor produced by CD31(−) CD45(−) SP cells that promotes proliferation of myoblasts, we extracted total RNAs from CD31(−) CD45(−) SP cells, myoblasts, and macrophages isolated from regenerating muscles 3 days after CTX injection, and examined the gene expression in these three cell populations by microarray. Eventually, we identified 192 genes that were expressed at more than 10-fold higher levels in CD31(−) CD45(−) SP cells than in either macrophages or myoblasts. We categorized the 192 genes based on gene ontology, and found that CD31(−) CD45(−) SP cells preferentially express extracellular matrix proteins and cytokines and their receptors (see Supplementary Table S1 at *http://ajp.amjpathol.org*). We found numerous genes involved in wound healing and tissue repair on the gene list, suggesting that CD31(−) CD45(−) SP cells play a regulatory role in the muscle regeneration process. Interestingly, the gene list contained both muscle prolif-

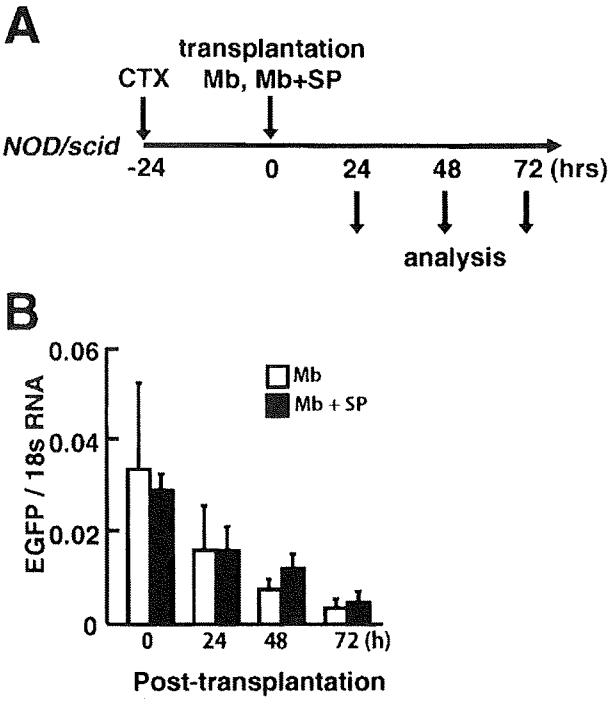

Figure 5. Survival of injected myoblasts in *NOD/scid* mice. **A:** Experimental design. GFP(+) myoblasts alone (3×10^4 cells) or a mixture of GFP(+) myoblasts (3×10^4 cells) and nonlabeled CD31(−) CD45(−) SP cells (2×10^4 cells) were injected into previously CTX-injected TA muscles of *NOD/scid* mice. The muscles were then sampled at 0, 24, 48, and 72 hours after transplantation. **B:** The mRNA level of GFP at each time point was quantified by real-time PCR. The *y* axis shows GFP mRNA levels normalized to 18s RNA with SE ($n = 4$ to 5).

eration or differentiation-promoting (follistatin),[26] and inhibitory factors (eg, insulin-like growth factor binding proteins,[27] Nov[28]). The list also contains regulators of TGF-β (eg, thrombospondins,[29] Prss11,[30] Ltbp3[31]), which would consequently attenuate or stimulate proliferation and differentiation of myoblasts.

CD31(−) CD45(−) SP Cell-Derived MMP-2 Promotes the Migration of Myoblasts

Genome-wide gene expression analysis revealed that CD31(−) CD45(−) SP cells highly express matrix metalloproteinases (see Supplementary Table S1 and Supplementary Figure S1 at *http://ajp.amjpathol.org*). MMPs are a group of zinc-dependent endopeptidases that degrade extracellular matrix components, thereby facilitating cell migration and tissue remodeling.[32,33] Furthermore, MMPs are known to release growth factors stored within the extracellular matrix and process growth factor receptors, resulting in stimulation of cell proliferation.[34–36] Among the MMPs up-regulated in CD31(−) CD45(−) SP cells, we paid special attention to MMP-2 (also called gelatinase A or 72-kDa type IV collagenase). In CTX-injected muscle, MMP-2 activity was shown to be increased concomitantly with the transition from the regeneration phases characterized by the appearance of young myotubes to maturation of the myotubes into multinucleated myofibers[37,38] MMP-2 was also activated in the endomysium of regenerating fibers in dystrophin-deficient muscular dystrophy dogs.[39] Furthermore, MMP-2 transcripts were found in the areas of fiber regeneration, and were localized to mesenchymal fibroblasts in DMD skeletal muscle.[40]

We confirmed that the mRNA level of MMP-2 was much higher in CD31(−) CD45(−) SP cells than in macrophages or myoblasts (Figure 7A). Next, we examined the gelatinolytic activity in CD31(−) CD45(−) SP cells, macrophages, and myoblasts by DQ-gelatin zymography. The cells were directly isolated from regenerating muscle. High gelatinolytic activity was detected in CD31(−) CD45(−) SP cells, compared to myoblasts or macrophages (Figure 7B). Importantly, the signal in MMP-2-null SP cells was considerably weak, compared with wild-type SP cells. The results indicate that DQ-gelatin was degraded mainly (but not exclusively) by MMP-2 in the assay. We hardly detected the green fluorescence in wild-type SP cells in the presence of a broad-spectrum inhibitor of MMPs, GM6001, but not a potent inhibitor of cysteine proteases, E-64, suggesting that other MMPs contribute to gelatin degradation to some extent in the assay. Collectively, these results indicate that CD31(−) CD45(−) SP cells have high MMP-2 activity.

MMP-2 is reported to mediate cell migration and tissue remodeling.[32,33] To directly investigate the effects of MMP-2 on the migration and proliferation of transplanted myoblasts, we injected GFP(+) myoblasts with CD31(−) CD45(−) SP cells prepared from wild-type mice or from MMP-2-null mice into CTX-injected TA muscles of *NOD/scid* mice. There was no difference in the yield of CD31(−) CD45(−) SP cells from regenerating muscle between wild-type and MMP-2-null mice (data not shown). Consistent with this observation, MMP-2-null CD31(−) CD45(−) SP cells proliferated as vigorously as wild-type *in vitro* (data not shown). At 72 hours after transplantation, GFP(+) myoblasts were more widely spread in the muscle co-injected with wild-type CD31(−) CD45(−) SP cells than in the muscles co-injected with MMP-2-deficient CD31(−) CD45(−) SP cells (Figure 7C). In contrast, there was no difference in the number of GFP(+) myoblasts between two groups (Figure 7D). These results strongly suggest that MMP-2 derived from CD31(−) CD45(−) SP cells significantly promotes migration of myoblasts, but does not influence the proliferation of myoblasts.

Discussion

We previously reported a novel SP subset: CD31(−) CD45(−) SP cells.[20] They are resident in skeletal muscle and are activated and vigorously proliferate during muscle regeneration. RT-PCR analysis suggested that CD31(−) CD45(−) SP cells are of mesenchymal lineage, and indeed they differentiated into adipocytes, osteogenic cells, and muscle cells after specific induction *in vitro*.[20] In the present study, we further characterized CD31(−) CD45(−) SP cells and found that co-transplantation of CD31(−) CD45(−) SP cells markedly improves the efficacy of myoblast transfer to dystrophic *mdx* mice. Our

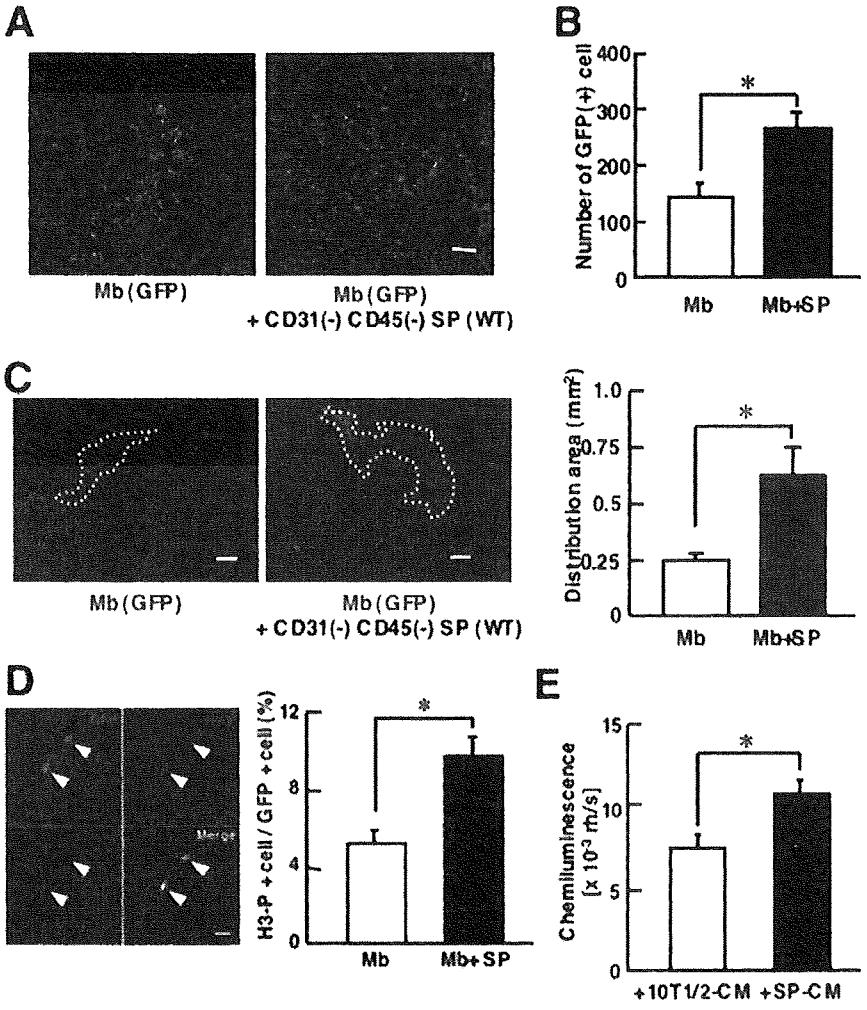

Figure 6. CD31(−) CD45(−) SP cells promote proliferation of myoblasts *in vitro* and *in vivo*. **A:** Representative images of cross sections of 72-hour samples stained with anti-GFP (green) and anti-laminin-α2 chain (red) antibodies. GFP(+) myoblasts are more widely scattered in injected muscle when co-transplanted with CD31(−) CD45(−) SP cells, compared with single transplantation. **B:** The number of GFP(+) cells per cross section of TA muscles injected with myoblasts or myoblasts and CD31(−) CD45(−) SP cells. Values were means with SE (n = 4 to 5). *$P < 0.05$. **C: Left:** Representative distributions of GFP(+) myoblasts/myotubes 72 hours after transplantation. **Right:** Distribution area (marked by white dotted lines in **left** panels) was measured by Image J software. Values were means with SE (n = 4 to 5). *$P < 0.05$. **D:** GFP(+) myoblasts were transplanted into CTX-injected TA muscles of *NOD/scid* mice with (Mb + SP) or without CD31(−) CD45(−) SP cells (Mb). Forty-eight hours after transplantation, the muscles were dissected, sectioned, and stained with anti-phosphorylated histone-H3 (H3-P) (red) and anti-GFP (green) antibodies. **Arrowheads** indicate H3-P(+) GFP(+) cells. The **right** graph shows the percentage of H3-P(+) cells in GFP(+) myoblasts in single-transplanted muscle (Mb) or in co-transplanted muscle (Mb + SP). The values are means with SE (n = 3). *$P < 0.05$. **E:** Myoblasts were cultured for 3 days in conditioned medium of either CD31(−) CD45(−) SP cells (SP-CM) or 10T1/2 cells (10T1/2-CM) and then cultured for an additional 24 hours in the presence of BrdU. The vertical axis shows BrdU uptake by myoblasts. Values are means with SE (n = 6). *$P < 0.05$. Scale bars: 100 μm (**A**); 200 μm (**C**); 80 μm (**D**).

findings suggest that endogenous CD31(−) CD45(−) SP cells support muscle regeneration by stimulating proliferation and migration of myoblasts.

Are CD31(−) CD45(−) SP Cells Mesenchymal Stem Cells?

Analysis of cell surface antigens on CD31(−) CD45(−) SP cells suggests that they are a homogeneous population. Several reports showed that mesenchymal stem cells (MSCs) express CD44, CD90, but not CD31, CD45, or CD14.[41,42] The expression patterns of these markers on CD31(−) CD45(−) SP cells and their differentiation potentials into osteogenic cells, adipocytes, and myogenic cells suggest that CD31(−) CD45(−) SP cells are closely related to MSCs.[20] On the other hand, the expression of PDGFRβ,[20] CD44, CD49b, CD90, and the lack of CD133 expression on CD31(−) CD45(−) SP cells are similar to those of human pericytes.[13] Unlike human pericytes, however, CD31(−) CD45(−) SP cells have limited myogenic potential *in vivo*.[13,20] The relationship between CD31(−) CD45(−) SP cells and MSCs or pericytes remains to be determined in a future study.

CD31(−) CD45(−) SP Cells Promote Proliferation of Myogenic Cells

In the present study, we demonstrated that the efficiency of myoblast transfer is greatly improved by co-transplantation of CD31(−) CD45(−) SP cells. Transplanted CD31(−) CD45(−) SP cells proliferated in the injection site and surrounded both engrafted myoblasts and damaged myofibers, but rarely fused with myoblasts (Figure 4). Transplantation of CD31(−) CD45(−) SP cells alone contributed little to myofiber formation. Therefore, the improvement in efficiency of myoblast transfer by co-transplantation is not attributable to differentiation of CD31(−) CD45(−) SP cells into muscle fibers.

Because the conditioned medium from CD31(−) CD45(−) SP cells modestly stimulated the proliferation of myoblasts *in vitro*, when compared with CM of 10T1/2 cells, it is possible that CD31(−) CD45(−) SP cells stimulated proliferation of myoblasts by secreting growth factors. CD31(−) CD45(−) SP cells are found in close vicinity to myoblasts 48 hours after transplantation. Therefore, even low levels of growth factors produced by CD31(−) CD45(−) SP cells may effectively stimulate the prolifera-

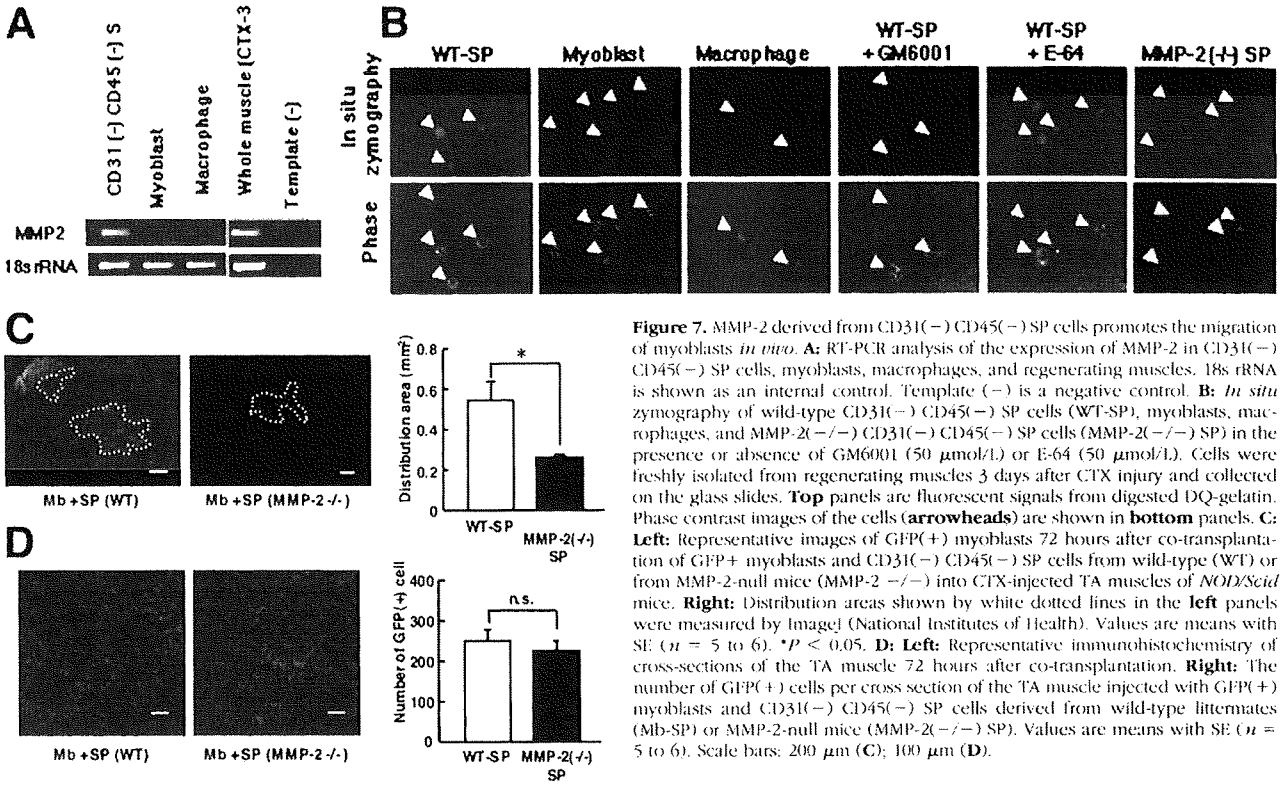

Figure 7. MMP-2 derived from CD31(−) CD45(−) SP cells promotes the migration of myoblasts *in vivo*. **A:** RT-PCR analysis of the expression of MMP-2 in CD31(−) CD45(−) SP cells, myoblasts, macrophages, and regenerating muscles. 18s rRNA is shown as an internal control. Template (−) is a negative control. **B:** *In situ* zymography of wild-type CD31(−) CD45(−) SP cells (WT-SP), myoblasts, macrophages, and MMP-2(−/−) CD31(−) CD45(−) SP cells (MMP-2(−/−) SP) in the presence or absence of GM6001 (50 μmol/L) or E-64 (50 μmol/L). Cells were freshly isolated from regenerating muscles 3 days after CTX injury and collected on the glass slides. **Top** panels are fluorescent signals from digested DQ-gelatin. Phase contrast images of the cells (**arrowheads**) are shown in **bottom** panels. **C: Left:** Representative images of GFP(+) myoblasts 72 hours after co-transplantation of GFP+ myoblasts and CD31(−) CD45(−) SP cells from wild-type (WT) or from MMP-2-null mice (MMP-2 −/−) into CTX-injected TA muscles of *NOD/Scid* mice. **Right:** Distribution areas shown by white dotted lines in the **left** panels were measured by ImageJ (National Institutes of Health). Values are means with SE (n = 5 to 6). *$P < 0.05$. **D: Left:** Representative immunohistochemistry of cross-sections of the TA muscle 72 hours after co-transplantation. **Right:** The number of GFP(+) cells per cross section of the TA muscle injected with GFP(+) myoblasts and CD31(−) CD45(−) SP cells derived from wild-type littermates (Mb-SP) or MMP-2-null mice (MMP-2(−/−) SP). Values are means with SE (n = 5 to 6). Scale bars: 200 μm (**C**); 100 μm (**D**).

tion of myoblasts. Importantly, several reports showed that MSCs secrete a variety of cytokines and growth factors, which suppress the local immune system, inhibit fibrosis and apoptosis, enhance angiogenesis, and stimulate mitosis and differentiation of tissue-specific stem cells.[43] On the gene list, we found a variety of cytokines/chemokines and their regulators (see Supplementary Table S1 at *http://ajp.amjpathol.org*). These molecules may directly or indirectly stimulate proliferation of myoblasts.

MMP-2 Derived from CD31(−) CD45(−) SP Cells Promotes the Migration of Myoblasts

Transplanted GFP(+) myoblasts were more widely spread in injected muscle when co-injected with CD31(−) CD45(−) SP cells than when transplanted alone (Figure 6C). MMP-2 is a candidate molecule that promotes migration of myoblasts. MMP-2 plays a critical role in myogenesis[44] and is up-regulated in muscle regeneration (see Supplementary Figure S2 at *http://ajp.amjpathol.org*).[38] MMP-2 expression is also detected in regenerating areas of dystrophic muscles.[39,40] Importantly, El Fahime and colleagues[45] reported that forced expression of MMP-2 in normal myoblasts significantly increased migration of myoblasts *in vivo*. In the present study, we demonstrated that CD31(−) CD45(−) SP cells highly express MMP-2 (see Figure 7A and Supplementary Table S1 at *http://ajp.amjpathol.org*). Gelatin zymography confirmed that CD31(−) CD45(−) SP cells have high gelatinolytic activities (Figure 7B). Importantly, CD31(−) CD45(−) SP cells prepared from wild-type mice promoted the migration of transplanted myoblasts, but those from MMP-2-null mice did not (Figure 7C). Our results suggest that CD31(−) CD45(−) SP cells promote the migration of myoblasts via MMP-2 secretion. CD31(−) CD45(−) SP cells highly express MMP-2, 3, 9, 14, and 23 during regenerating muscle (see Supplementary Figures S1 and S2 and Supplementary Table S1 at *http://ajp.amjpathol.org*). Therefore, it remains to be determined whether MMPs other than MMP-2 also promote the migration of myoblasts. MMPs are reported to promote cell proliferation by releasing local growth factors stored within the extracellular matrix and process growth factor receptors.[34,35,46] In the present study, however, MMP-2 derived from CD31(−) CD45(−) SP cells did not stimulate the proliferation of myoblasts *in vivo* (Figure 7D). The factors that stimulate the proliferation of myoblasts remain to be determined in a future study. MMP-3, -9, -14, and -23 are candidates that play a role in stimulating the proliferation of myoblasts.

CD31(−) CD45(−) SP Cells Are the Third Cellular Component of Muscle Regeneration

Our results suggest that transplanted CD31(−) CD45(−) SP cells stimulate myogenesis of co-transplanted myoblasts by supporting their proliferation and migration. Our results also suggest that endogenous CD31(−) CD45(−) SP cells promote muscle regeneration by the same mechanisms. Muscle regeneration is a complex, highly coordinated process in which not only myogenic cells but also inflammatory cells such as macrophages play critical roles.[3] Based on our finding that CD31(−) CD45(−) SP cells regulate myoblast proliferation and migration, we

propose that CD31(−) CD45(−) SP cells are a third cellular component of muscle regeneration. In addition, gene expression analysis on CD31(−) CD45(−) SP cells revealed that CD31(−) CD45(−) SP cells express a wide range of regulatory molecules implicated in embryonic development, tissue growth and repair, angiogenesis, and tumor progression, suggesting that CD31(−) CD45(−) SP cells are a versatile player in regeneration of skeletal muscle. Future studies of ablation of endogenous CD31(−) CD45(−) SP cells in the mouse will likely further clarify the mechanisms by which CD31(−) CD45(−) SP cells promote muscle regeneration.

Acknowledgments

We thank Satoru Masuda and Chika Harano for technical support.

References

1. Chargé SB, Rudnicki MA: Cellular and molecular regulation of muscle regeneration. Physiol Rev 2004, 84:209–238
2. Orimo S, Hiyamuta E, Arahata K, Sugita H: Analysis of inflammatory cells and complement C3 in bupivacaine-induced myonecrosis. Muscle Nerve 1991, 14:515–520
3. Tidball JG: Inflammatory processes in muscle injury and repair. Am J Physiol 2005, 288:R345–R353
4. Mauro A: Satellite cell of skeletal muscle fibers. J Biophys Biochem Cytol 1961, 9:493–495
5. Collins CA, Olsen I, Zammit PS, Heslop L, Petrie A, Partridge TA, Morgan JE: Stem cell function, self-renewal, and behavioral heterogeneity of cells from the adult muscle satellite cell niche. Cell 2005, 122:289–301
6. Kuang S, Kuroda K, Le Grand F, Rudnicki MA: Asymmetric self-renewal and commitment of satellite stem cells in muscle. Cell 2007, 129:999–1010
7. Qu-Petersen Z, Deasy B, Jankowski, R, Ikezawa M, Cummins J, Pruchnic R, Mytinger J, Cao B, Gates C, Wernig A, Huard J: Identification of a novel population of muscle stem cells in mice: potential for muscle regeneration. J Cell Biol 2002, 157:851–864
8. Jiang Y, Vaessen B, Lenvik T, Blackstad M, Reyes M, Verfaillie CM: Multipotent progenitor cells can be isolated from postnatal murine bone marrow, muscle, and brain. Exp Hematol 2002, 30:896–904
9. Tamaki T, Akatsuka A, Ando K, Nakamura Y, Matsuzawa H, Hotta T, Roy RR, Edgerton VR: Identification of myogenic-endothelial progenitor cells in the interstitial spaces of skeletal muscle. J Cell Biol 2002, 157:571–577
10. Torrente Y, Tremblay JP, Pisati F, Belicchi M, Rossi B, Sironi M, Fortunato F, El Fahime M, D'Angelo MG, Caron NJ, Constantin G, Paulin D, Scarlato G, Bresolin N: Intraarterial injection of muscle-derived CD34(+)Sca-1(+) stem cells restores dystrophin in mdx mice. J Cell Biol 2001, 152:335–348
11. Polesskaya A, Seale P, Rudnicki MA: Wnt signaling induces the myogenic specification of resident CD45+ adult stem cells during muscle regeneration. Cell 2003, 113:841–852
12. Sampaolesi M, Blot S, D'Antona G, Granger N, Tonlorenzi R, Innocenzi A, Mognol P, Thibaud JL, Galvez BG, Barthelemy I, Perani L, Mantero S, Guttinger M, Pansarasa O, Rinaldi C, Cusella De Angelis MG, Torrente Y, Bordignon C, Bottinelli R, Cossu G: Mesoangioblast stem cells ameliorate muscle function in dystrophic dogs. Nature 2006, 444:574–579
13. Dellavalle A, Sampaolesi M, Tonlorenzi R, Tagliafico E, Sacchetti B, Perani L, Innocenzi A, Galvez BG, Messina G, Morosetti R, Li S, Belicchi M, Peretti G, Chamberlain JS, Wright WE, Torrente Y, Ferrari S, Bianco P, Cossu G: Pericytes of human skeletal muscle are myogenic precursors distinct from satellite cells. Nat Cell Biol 2007, 9:255–267
14. Goodell MA, Brose K, Paradis G, Conner AS, Mulligan RC: Isolation and functional properties of murine hematopoietic stem cells that are replicating in vivo. J Exp Med 1996, 183:1797–1806
15. Gussoni E, Soneoka Y, Strickland CD, Buzney EA, Khan MK, Flint AF, Kunkel LM, Mulligan RC: Dystrophin expression in the mdx mouse restored by stem cell transplantation. Nature 1999, 401:390–394
16. Jackson KA, Mi T, Goodell MA: Hematopoietic potential of stem cells isolated from murine skeletal muscle. Proc Natl Acad Sci USA 1999, 96:14482–14486
17. Asakura A, Seale P, Girgis-Gabardo A, Rudnicki MA: Myogenic specification of side population cells in skeletal muscle. J Cell Biol 2002, 159:123–134
18. Bachrach E, Perez AL, Choi YH, Illigens BM, Jun SJ, del Nido P, McGowan FX, Li S, Flint A, Chamberlain J: Muscle engraftment of myogenic progenitor cells following intraarterial transplantation. Muscle Nerve 2006, 34:44–52
19. Frank NY, Kho AT, Schatton T, Murphy GF, Molloy MJ, Zhan Q, Ramoni MF, Frank MH, Kohane IS, Gussoni E: Regulation of myogenic progenitor proliferation in human fetal skeletal muscle by BMP4 and its antagonist Gremlin. J Cell Biol 2006, 175:99–110
20. Uezumi A, Ojima K, Fukada S, Ikemoto M, Masuda S, Miyagoe-Suzuki Y, Takeda S: Functional heterogeneity of side population cells in skeletal muscle. Biochem Biophys Res Commun 2006, 341:864–873
21. Ojima K, Uezumi A, Miyoshi H, Masuda S, Morita Y, Fukase A, Hattori A, Nakauchi H, Miyagoe-Suzuki Y, Takeda S: Mac-1(low) early myeloid cells in the bone marrow-derived SP fraction migrate into injured skeletal muscle and participate in muscle regeneration. Biochem Biophys Res Commun 2004, 321:1050–1061
22. Itoh T, Ikeda T, Gomi H, Nakao S, Suzuki T, Itohara S: Unaltered secretion of β-amyloid precursor protein in gelatinase A (matrix metalloproteinase 2)-deficient mice. J Biol Chem 1997, 272:22389–22392
23. Fukada S, Higuchi S, Segawa M, Koda K, Yamamoto Y, Tsujikawa K, Kohama Y, Uezumi A, Imamura M, Miyagoe-Suzuki Y, Takeda S, Yamamoto H: Purification and cell-surface marker characterization of quiescent satellite cells from murine skeletal muscle by a novel monoclonal antibody. Exp Cell Res 2004, 296:245–255
24. Kitamura T, Koshino Y, Shibata F, Oki T, Nakajima H, Nosaka T, Kumagai H: Retrovirus-mediated gene transfer and expression cloning: powerful tools in functional genomics. Exp Hematol 2003, 31:1007–1014
25. Morita S, Kojima T, Kitamura T: Plat-E: an efficient and stable system for transient packaging of retroviruses. Gene Ther 2000, 7:1063–1066
26. Lee SJ, McPherron AC: Regulation of myostatin activity and muscle growth. Proc Natl Acad Sci USA 2001, 98:9306–9311
27. Holly J, Perks C: The role of insulin-like growth factor binding proteins. Neuroendocrinology 2006, 83:154–160
28. Sakamoto K, Yamaguchi S, Ando R, Miyawaki A, Kabasawa Y, Takagi M, Li CL, Perbal B, Katsube K: The nephroblastoma overexpressed gene (NOV/ccn3) protein associates with Notch1 extracellular domain and inhibits myoblast differentiation via Notch signaling pathway. J Biol Chem 2002, 277:29399–29405
29. Lawler J: The functions of thrombospondin-1 and-2. Curr Opin Cell Biol 2000, 12:634–640
30. Tocharus J, Tsuchiya A, Kajikawa M, Ueta Y, Oka C, Kawaichi M: Developmentally regulated expression of mouse HtrA3 and its role as an inhibitor of TGF-beta signaling. Dev Growth Differ 2004, 46:257–274
31. Colarossi C, Chen Y, Obata H, Jurukovski V, Fontana L, Dabovic B, Rifkin DB: Lung alveolar septation defects in Ltbp-3-null mice. Am J Pathol 2005, 167:419–428
32. McCawley LJ, Matrisian LM: Matrix metalloproteinases: they're not just for matrix anymore! Curr Opin Cell Biol 2001, 13:534–540
33. Balcerzak D, Querengesser L, Dixon WT, Baracos VE: Coordinate expression of matrix-degrading proteinases and their activators and inhibitors in bovine skeletal muscle. J Anim Sci 2001, 79:94–107
34. Kayagaki N, Kawasaki A, Ebata T, Ohmoto H, Ikeda S, Inoue S, Yoshino K, Okumura K, Yagita H: Metalloproteinase-mediated release of human Fas ligand. J Exp Med 1995, 182:1777–1783
35. Lanzrein M, Garred O, Olsnes S, Sandvig K: Diphtheria toxin endocytosis and membrane translocation are dependent on the intact membrane-anchored receptor (HB-EGF precursor): studies on the cell-associated receptor cleaved by a metalloprotease in phorbol-ester-treated cells. Biochem J 1995, 310:285–289
36. Couch CB, Strittmatter WJ: Rat myoblast fusion requires metalloendoprotease activity. Cell 1983, 32:257–265

37. Ohtake Y, Tojo H, Seiki M: Multifunctional roles of MT1-MMP in myofiber formation and morphostatic maintenance of skeletal muscle. J Cell Sci 2006, 119:3822–3832
38. Kherif S, Lafuma C, Dehaupas M, Lachkar S, Fournier JG, Verdière-Sahuqué M, Fardeau M, Alameddine HS: Expression of matrix metalloproteinases 2 and 9 in regenerating skeletal muscle: a study in experimentally injured and mdx muscles. Dev Biol 1999, 205:158–170
39. Fukushima K, Nakamura A, Ueda H, Yuasa K, Yoshida K, Takeda S, Ikeda S: Activation and localization of matrix metalloproteinase-2 and -9 in the skeletal muscle of the muscular dystrophy dog (CXMDJ). BMC Musculoskelet Disord 2007, 8:54
40. von Moers A, Zwirner A, Reinhold A, Brückmann O, van Landeghem F, Stoltenburg-Didinger G, Schuppan D, Herbst H, Schuelke M: Increased mRNA expression of tissue inhibitors of metalloproteinase-1 and -2 in Duchenne muscular dystrophy. Acta Neuropathol (Berl) 2005, 109:285–293
41. Pittenger MF, Mackay AM, Beck SC, Jaiswal RK, Douglas R, Mosca JD, Moorman MA, Simonetti DW, Craig S, Marshak DR: Multilineage potential of adult human mesenchymal stem cells. Science 1999, 284:143–147
42. Conget PA, Minguell JJ: Phenotypical and functional properties of human bone marrow mesenchymal progenitor cells. J Cell Physiol 1999, 181:67–73
43. Caplan AI, Dennis JE: Mesenchymal stem cells as trophic mediators. J Cell Biochem 2006, 98:1076–1084
44. Oh J, Takahashi R, Adachi E, Kondo S, Kuratomi S, Noma A, Alexander DB, Motoda H, Okada A, Seiki M, Itoh T, Itohara S, Takahashi C, Noda M: Mutations in two matrix metalloproteinase genes, MMP-2 and MT1-MMP, are synthetic lethal in mice. Oncogene 2004, 23:5041–5048
45. El Fahime E, Torrente Y, Caron NJ, Bresolin MD, Tremblay JP: In vivo migration of transplanted myoblasts requires matrix metalloproteinase activity. Exp Cell Res 2000, 258:279–287
46. Gearing AJ, Beckett P, Christodoulou M, Churchill M, Clements J, Davidson AH, Drummond AH, Galloway WA, Gilbert R, Gordon JL, Leber TM, Mangan M, Miller K, Nayee P, Owen K, Patel S, Thomas W, Wells G, Wood LM, Woolley K: Processing of tumour necrosis factor-alpha precursor by metalloproteinases. Nature 1994, 370:555–557

HUMAN GENE THERAPY 19:719–730 (July 2008)

DOI: 10.1089/hum.2007.184

Recombinant Adeno-Associated Virus Type 8-Mediated Extensive Therapeutic Gene Delivery into Skeletal Muscle of α-Sarcoglycan-Deficient Mice

Akiyo Nishiyama,[1] Beryl Nyamekye Ampong,[1] Sachiko Ohshima,[1] Jin-Hong Shin,[1] Hiroyuki Nakai,[2] Michihiro Imamura,[1] Yuko Miyagoe-Suzuki,[1] Takashi Okada,[1] and Shin'ichi Takeda[1]

Abstract

Autosomal recessive limb-girdle muscular dystrophy type 2D (LGMD 2D) is caused by mutations in the α-sarcoglycan gene (α-SG). The absence of α-SG results in the loss of the SG complex at the sarcolemma and compromises the integrity of the sarcolemma. To establish a method for recombinant adeno-associated virus (rAAV)-mediated α-SG gene therapy into α-SG-deficient muscle, we constructed rAAV serotypes 2 and 8 expressing the human α-SG gene under the control of the ubiquitous cytomegalovirus promoter (rAAV2-α-SG and rAAV8-α-SG). We compared the transduction profiles and evaluated the therapeutic effects of a single intramuscular injection of rAAVs into α-SG-deficient ($Sgca^{-/-}$) mice. Four weeks after rAAV2 injection into the tibialis anterior (TA) muscle of 10-day-old $Sgca^{-/-}$ mice, transduction of the α-SG gene was localized to a limited area of the TA muscle. On the other hand, rAAV8-mediated α-SG expression was widely distributed in the hind limb muscle, and persisted for 7 months without inducing cytotoxic and immunological reactions, with a reversal of the muscle pathology and improvement in the contractile force of the $Sgca^{-/-}$ muscle. This extensive rAAV8-mediated α-SG transduction in LGMD 2D model animals paves the way for future clinical application.

Introduction

Limb-girdle muscular dystrophy type 2D (LGMD 2D) is caused by mutations in the α-sarcoglycan (α-SG) gene, and is the most frequent cause of the autosomal recessive LGMD. LGMD 2D patients have the clinical characteristics of progressive muscle necrosis in the proximal limb muscles (Eymard *et al.*, 1997). Sarcoglycans (SGs) are essential constituents of the dystrophin-associated protein (DAP) complex, which consists of several membrane-spanning and cytoplasmic proteins, including dystroglycans (α and β), SGs (α, β, γ, and δ), sarcospan, syntrophins (α_1, β_1, and β_2), and dystrobrevins that directly or indirectly associate with dystrophin (Ervasti *et al.*, 1990; Yoshida and Ozawa, 1990; Iwata *et al.*, 1993). A defect in any one of the four SGs can disrupt the entire SG complex. Mutations in four genes encoding α-, β-, γ-, and δ-SG are responsible for autosomal recessive LGMD 2D, 2E, 2C and 2F, respectively (Ervasti *et al.*, 1990; Bonnemann *et al.*, 1995; Noguchi *et al.*, 1995; Nigro *et al.*, 1996; Eymard *et al.*, 1997; Fanin *et al.*, 1997).

Many *in vivo* studies have demonstrated that recombinant adeno-associated virus (rAAV) packaged in various serotypes of AAV capsids exhibits serotype-specific tissue or cell tropism with different transduction efficiencies (Fisher *et al.*, 1997; Greelish *et al.*, 1999; Gao *et al.*, 2002, 2004; Wang *et al.*, 2005). rAAV has been shown to mediate long-term transgene expression in many tissues without evoking severe immune reactions. Some rAAVs efficiently transduce skeletal muscle (Kessler *et al.*, 1996; Xiao *et al.*, 1996; Fisher *et al.*, 1997). rAAV serotype 2 (rAAV2)-mediated muscle gene therapy is a promising approach, but it is effective only locally. In contrast, rAAV serotype 8 (rAAV8)-mediated gene transfer is capable of crossing capillary blood vessels to achieve systemic gene delivery, and effectively transduces genes into cardiac and skeletal muscle (Wang *et al.*, 2005). Therefore, rAAV8 is a good candidate for a therapeutic tool.

To assess the efficacy and therapeutic potential of rAAV8 for LGMD 2D, we directly injected rAAV2-α-SG and rAAV8-α-SG into the tibialis anterior (TA) muscles of 10-day-old α-SG-deficient mice (neonatal $Sgca^{-/-}$ mice). Our data suggested not

[1]Department of Molecular Therapy, National Institute of Neuroscience, National Center of Neurology and Psychiatry, Tokyo 187-8502, Japan.
[2]Department of Molecular Genetics and Biochemistry, University of Pittsburgh School of Medicine, Pittsburgh, PA 15261.

only the extensive expression of α-SG in Sgca $^{-/-}$ skeletal muscle, but also a robust level of expression of α-SG at the sarcolemma after a single intramuscular injection of rAAV8-α-SG. In addition, rAAV8-α-SG effectively transduced the cardiac muscle of 7-week-old Sgca $^{-/-}$ mice (adult Sgca $^{-/-}$ mice). Most importantly, 7 months after the injection of rAAV8-α-SG into neonatal Sgca $^{-/-}$ mice, expression of α-SG and improvement of sarcolemmal function were sustained, without inducing cytotoxic and immunological reactions. Thus, the AAV8 vector is a promising tool for gene therapy of LGMD 2D.

Materials and Methods

Recombinant AAV production

The full-length human α-SG cDNA was amplified from a skeletal muscle single-strand cDNA library (Human Skeletal Muscle Marathon-Ready cDNA; Clontech, Palo Alto, CA) by polymerase chain reaction (PCR) with the following set of oligonucleotide primers: 5′-CTCTGTCACTCACCGGG-3′ (nucleotide positions 2–18) and 5′-AGGATGAAGTC-AGGGCTGGAC-3′ (nucleotide positions 1223–1243) (McNally *et al.*, 1994). The amplification was carried out with LA-Taq polymerase (TaKaRa Bio, Shiga, Japan) for 30 cycles, with each cycle consisting of 94°C for 30 sec and 60°C for 2 min. The PCR products were then cloned into a TA cloning vector (Invitrogen, Carlsbad, CA), and sequenced with an ABI310 sequencer (Applied Biosystems, Foster City, CA). α-SG cDNA was then cloned into an AAV serotype 2 vector plasmid (Xiao *et al.*, 1998; Yuasa *et al.*, 2002) including the cytomegalovirus (CMV) promoter, splicing donor/acceptor (SD/SA) sites derived from the simian virus 40 (SV40), an SV40 poly(A) signal, inverted terminal repeat (ITR) of the AAV2 viral genome, and 2.0 kb of λ DNA, which served as a stuffer (depicted in Fig. 1A).

The vector genome was packaged in the AAV2 capsid or pseudotyped into the AAV8 capsid by triple transfection of

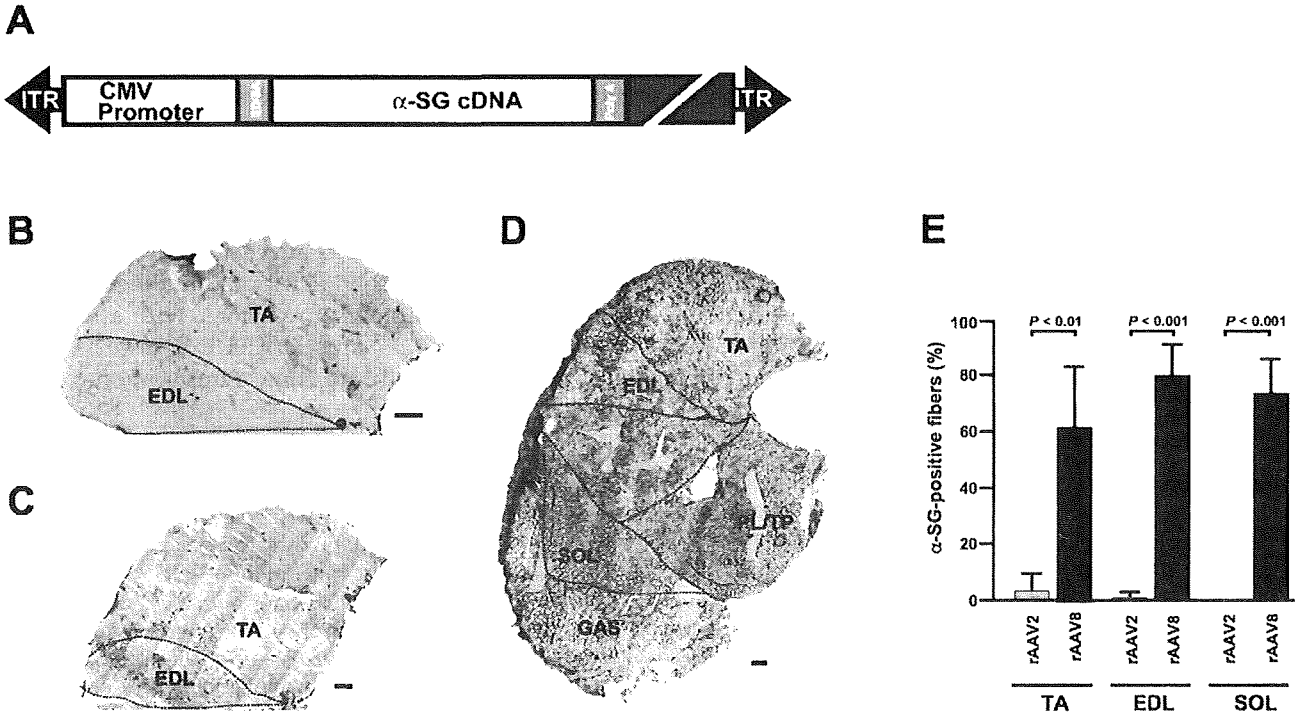

FIG. 1. Widespread expression of α-SG in hind limb muscles after a single injection of rAAV2-α-SG or rAAV8-α-SG into the tibialis anterior (TA) muscles of 10-day-old α-SG-deficient mice. (**A**) Genomic structure of rAAV used in this study. Human α-SG cDNA (1.2 kb) was inserted downstream of the CMV promoter. ITR, inverted terminal repeat from AAV2 genome; SD/SA, splicing donor/acceptor sites derived from SV40 intron; poly(A), a polyadenylation signal from SV40. The large shaded box represents a stuffer sequence derived from λ DNA. (**B–D**) Right TA muscles of neonatal Sgca $^{-/-}$ mice were injected with 1×10^{11} VG of rAAV2-α-SG (**C**) or rAAV8-α-SG (**D**). Four weeks after rAAV injection, the hind limb muscles of Sgca $^{-/-}$ mice were immunolabeled with a rabbit polyclonal antibody to α-SG. Hind limb muscles included the TA, extensor digitorum longus (EDL), plantaris (PL)/tibialis posterior (TP), soleus (SOL), and gastrocnemius (GAS) muscles. The TA and EDL muscles of Sgca $^{-/-}$ mice are shown as negative controls (**B**). Note that α-SG is expressed not only in rAAV8-injected TA muscle, but also in all hind limb muscles after direct injection of rAAV8-α-SG into the right TA muscle (**D**). Scale bars (**B–D**): 500 μm. (**E**) Percentages of α-SG-positive myofibers in TA, EDL, and SOL muscles after injection of rAAV2-α-SG (shaded columns) and rAAV8-α-SG (solid columns) injection into TA muscles of Sgca $^{-/-}$ mice. The right TA muscles of neonatal Sgca $^{-/-}$ mice were transduced with 1×10^{11} VG of rAAV2-α-SG or rAAV8-α-SG. Four weeks after rAAV injection, the hind limb muscles of Sgca $^{-/-}$ mice were immunolabeled with the α-SG antibody and then counterstained with hematoxylin and eosin. Hind limb muscles include the TA, EDL, and SOL muscles. The percentage of α-SG-positive myofibers was calculated on the basis of more than 200 total myofibers in cross-sections from three animals for each group. p Values are indicated and show statistical significance between Sgca $^{-/-}$ mice and rAAV8-injected Sgca $^{-/-}$ mice ($p < 0.01$ for TA, $p < 0.001$ for EDL, and $p < 0.001$ for SOL).

the AAV vector plasmid, AAV helper plasmid (p5E18-VD2/8) (Wang *et al.*, 2005), and adenovirus helper plasmid (XX6) (Xiao *et al.*, 1998) at a molecular ratio of 1:1:1 in 293 cells, using the calcium phosphate coprecipitation method (Wigler *et al.*, 1980). All the vectors were then purified by two cycles of cesium chloride gradient centrifugation, and concentrated as described by Burton and coworkers (1999). The final viral preparations were kept in phosphate-buffered saline. Physical particle titers were determined by a quantitative dot-blot assay.

Administration of rAAV vectors to murine skeletal muscle

All animal-handling procedures were done in accordance with a protocol approved by the committee of the National Institute of Neuroscience (National Center of Neurology and Psychiatry, Kodaira, Japan). Wild-type ($Sgca^{+/+}$) and $Sgca^{-/-}$ mice (Burnham Institute, La Jolla, CA) were used. The TA muscles of 10-day-old (neonate) and 7-week-old (adult) $Sgca^{-/-}$ mice were transduced with 1×10^{11} vector genomes (VG) (10 μl) and 5×10^{11} VG (50 μl), respectively, of rAAV2- or rAAV8-α-SG, using 29-gauge needles.

Transgene expression analyses

Histological and immunohistochemical analyses were performed as described (Imamura *et al.*, 2000; Yuasa *et al.*, 2002). Cryosections (6 μm thick) were prepared from frozen muscle.

For colorimetric immunodetection of α-SG, blocked cryosections were incubated with a 1:1000 dilution of rabbit polyclonal anti-α-SG (Araishi *et al.*, 1999) for 1 hr at room temperature. The signal was visualized with a VECTASTAIN ABC kit (Vector Laboratories, Burlingame, CA) and then counterstained with hematoxylin and eosin (H&E). Stained sections were photographed with a light microscope (Leica, Heidelberg, Germany) using DP70 image scanning software (Olympus, Tokyo, Japan).

For fluorescence immunohistochemical detection of SGs, cryosections were fixed by immersion in cold acetone at −20°C for 5 min. After blocking with 2% casein in Tris-buffered saline (TBS, pH 7.4) at room temperature for 1 hr, α-SG was detected with rabbit polyclonal anti-α-SG (1:1000 dilution) (Araishi *et al.*, 1999). β-, γ-, and δ-SGs were detected with mouse monoclonal anti-β-SG (NCL-b-SARC, 1:50 dilution; Novocastra Laboratories, Newcastle-upon-Tyne, UK), anti-γ-SG (1:50 dilution), and anti-δ-SG (DSG-1; 1:50 dilution), respectively, after blocking with an M.O.M. kit (Vector Laboratories). Mouse monoclonal antibodies against γ-SG and δ-SG (DSG-1) were generated in our laboratory (Yamamoto *et al.*, 1994; Noguchi *et al.*, 1999). The signal was visualized with Alexa 488-conjugated anti-rabbit and anti-mouse IgG antibodies (Invitrogen Molecular Probes, Eugene, OR). Fluorescence signals were observed with a confocal laser-scanning microscope (Leica TCS SP; Leica).

Sodium dodecyl sulfate–polyacrylamide gel electrophoresis (SDS–PAGE) and protein transfer to a polyvinylidene di-

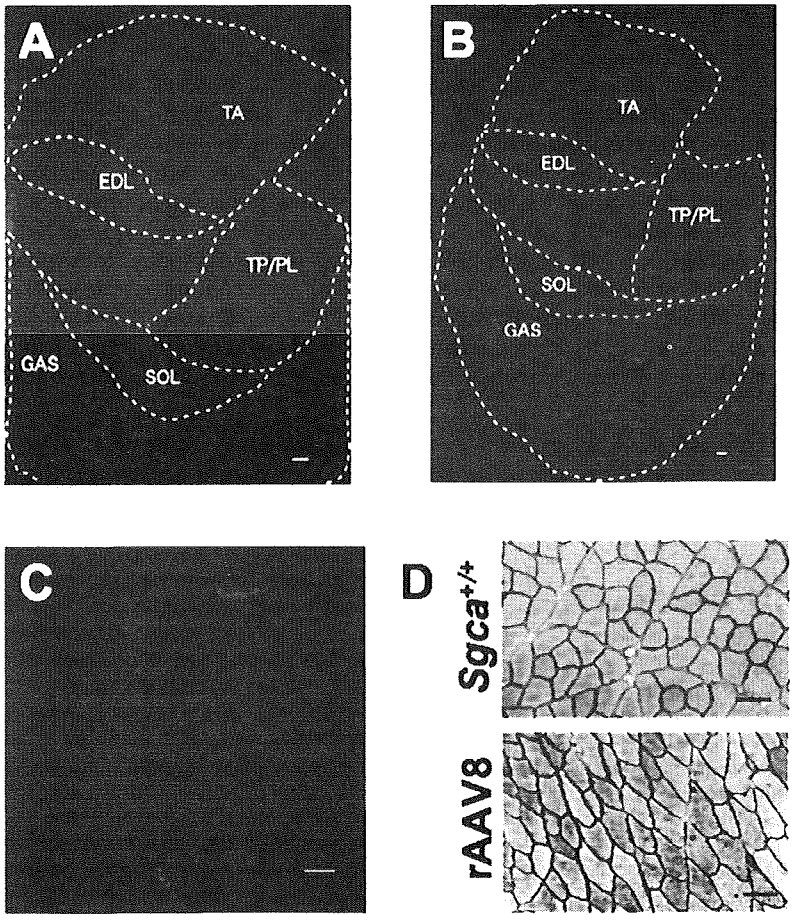

FIG. 2. Extensive α-SG expression after injection of rAAV8-α-SG into TA muscles of 7-week-old α-SG-deficient mice. Right TA muscles of adult $Sgca^{-/-}$ or $Sgca^{+/+}$ mice were transduced with 5×10^{11} VG of rAAV8-α-SG. Four weeks after rAAV8 injection, a cross-section of the right hind limb muscles (rAAV8-injected) (**A**), left contralateral hind limb muscles (**B**), and cardiac apex (**C**) were labeled by indirect immunofluorescence, using α-SG antibody (green). Scale bars: (**A** and **B**) 500 μm; (**C**) 100 μm. Note the widespread expression of α-SG in the hind limb muscles and cardiac muscle of rAAV8-α-SG-injected mice. (**D**) Cross-sections of TA muscle from $Sgca^{+/+}$ and rAAV8-injected $Sgca^{-/-}$ (rAAV8) mice were immunolabeled with α-SG antibody and counterstained with hematoxylin and eosin. Overexpression of α-SG caused no cytotoxic reactions in $Sgca^{+/+}$ muscle. Scale bars (**D**): 50 μm.

fluoride (PVDF) membrane were performed as described by Laemmli (1970) and Kyhse-Andersen (1984), respectively. Protein concentrations were determined with a protein assay kit (Bio-Rad, Hercules, CA) with bovine serum albumin as a standard.

Transgene copy number analyses

Cryosections of mouse hind limb muscle were collected for vector copy number analysis by quantitative PCR. After DNA extraction by successive treatments with RNase and proteinase K, viral genomes were quantified by a real-time PCR assay using SYBR *Premix Ex Taq* (TaKaRa Bio). The real-time PCR was carried out for 40 cycles, with each cycle consisting of 95°C for 5 sec, 60°C for 10 sec, 72°C for 10 sec, and 75°C for 10 sec. Oligonucleotide primers for this assay were 5′-CTCTAGAGGATCCGGTACTCGAGGAAC-3′ (SD/SA sites) and 5′-AGAGGAGTCCAGAAGAGTGTCTCAGCC-3′ (human α-SG gene) for the α-SG gene in the rAAV2 genome and 5′-TGCCATGAGCAGCCCATTTTG-3′ and 5′-ATAACATCGCGGTGGCTCAGG-3′ for the slug promoter. The slug promoter was used for normalization of data across samples.

Analysis of toxicity

Blood was obtained from a murine heart. Serum alanine aminotransferase, γ-glutamyl transpeptidase, albumin, and total protein concentration were determined with a Fuji Dri-Chem slide system (Fujifilm, Tokyo, Japan).

Muscle physiological function

TA and extensor digitorum longus (EDL) muscles were exposed by removal of overlying connective tissue (Xiao *et al.*, 2000; Yoshimura *et al.*, 2004; Imamura *et al.*, 2005). Both tendons of the TA and EDL muscles were cut from their insertions and secured with 5-0 silk sutures. Muscles were mounted in a vertical tissue chamber containing physiological salt solution (150 m*M* NaCl, 4 m*M* KCl, 1.8 m*M* $CaCl_2$, 1 m*M* $MgCl_2$, 5 m*M* HEPES, 5.6 m*M* glucose [pH 7.4], and 0.02 m*M* D-tubocurarine) maintained at 37°C with continuous aeration. The chamber was connected to a force transducer (UL-10GR; Minerva, Nagano, Japan) and a length servosystem (MM-3; Narishige, Tokyo, Japan). Electrical stimulation (SEN3301; Nihon Kohden, Tokyo, Japan) was delivered through a pair of platinum wires placed on both sides of the muscle. The muscle fiber length was adjusted incrementally with a micropositioner until peak isometric twitch force responses were obtained (i.e., optimal fiber length L_o). L_o was measured with a microcaliper. Maximal tetanic force (P_o) was induced by stimulation frequencies of 125 pulses per second, delivered in trains of 500-msec duration with 2-min intervals between each train. The muscle was weighed, rapidly frozen in liquid nitrogen-cooled isopentane, and stored at –80°C for further analysis. All forces were normalized to the physiological cross-section area (CSA), which was estimated on the basis of the following formula: muscle wet weight (in mg)/[L_o (in mm) × 1.06 (in mg/mm^3)]. The estimated CSA was used to determine specific tetanic (P_o/CSA) force of the muscle. Data are presented as means ± SE. Differences between groups were assessed by Student *t* test.

Exercise tolerance tests

Mice were subjected to an exhaustion treadmill test (Mourkioti *et al.*, 2006). Each mouse was placed on the belt of a four-lane motorized treadmill (MK-680; Muromachi Kikai, Tokyo, Japan) supplied with shocker plates. The treadmill was run at an inclination of 7 degrees at 5 m/min for 5 min, after which the speed was increased by 1 m/min every minute. The test was terminated when the mouse remained on the shocker plate for more than 20 sec without attempting to reengage the treadmill, and the time to exhaustion was determined.

Results

Expression of α-SG after injection of rAAV2- or rAAV8-α-SG into TA muscles of neonatal α-SG-deficient mice

We constructed rAAV2- and rAAV8-α-SG expressing human α-SG cDNA under the control of the ubiquitous CMV promoter, and injected 1×10^{11} VG into the right TA muscle of neonatal Sgca$^{-/-}$ mice (Fig. 1A). Neonatal Sgca$^{-/-}$ mice showed no obvious dystrophic changes, whereas adult (>4 weeks old) Sgca$^{-/-}$ skeletal muscles showed active cycles of the degeneration–regeneration process. In the hind limb muscles of 5-week-old Sgca$^{-/-}$ mice, α-SG-positive

TABLE 1. EFFECT OF rAAV2- AND rAAV8-α-SARCOGLYCAN ADMINISTRATION ON THE LIVER FUNCTION OF ADULT Sgca$^{-/-}$ MICE 4 WEEKS AFTER INJECTION[a,b]

	Number of mice	*ALT (U/liter)*	*γ-GTP (U/liter)*	*ALB (g/dl)*	*TP (g/dl)*
Sgca$^{+/+}$	3	26.67 ± 8.50[c]	<10	2.43 ± 0.21	4.80 ± 0.20
Sgca$^{-/-}$	3	145.33 ± 22.22	<10	2.33 ± 0.23	4.60 ± 0.42
rAAV2-injected Sgca$^{-/-}$	3	149 ± 9[d]	<10	2.10 ± 0.44	4.00 ± 0.53
rAAV8-injected Sgca$^{-/-}$	3	124 ± 15.10[e]	<10	2.03 ± 0.25	4.60 ± 0.89

Abbreviations: ALT/GPT, alanine aminotransferase/glutamic pyruvic transaminase; γ-GTP, γ-glutamyl transpeptidase; ALB, albumin; TP, total protein.

[a]Data represent means ± SE.

[b]The *p* values indicate statistical significance. Significant differences from the ALT/GPT level of Sgca$^{-/-}$ mice are indicated.

[c]$p < 0.001$.

[d]$p = 0.797$.

[e]$p = 0.229$.

fibers were not observed and the active cycle of muscle degeneration–regeneration was present (Fig. 1B). Four weeks after a single intramuscular injection of rAAV2-α-SG, α-SG was expressed only in a limited area of rAAV2-injected TA muscle (Fig. 1C and E). Analysis of TA muscle showed that less than 10% of muscle fibers were α-SG positive ($p < 0.01$; Fig. 1E).

In contrast, after rAAV8-α-SG injection, α-SG-positive fibers were widely spread in rAAV8-injected hind limb muscles, including the TA, extensor digitorum longus (EDL), soleus (SOL), gastrocnemius (GAS), and plantaris (PL)/tibialis posterior (TP) muscles (Fig. 1D). Analysis of the TA, EDL, and SOL muscles showed 62.3 ± 20.2, 79.5 ± 11.0, and 74.2 ± 11.2% α-SG-positive fibers, respectively ($p < 0.01$, $p < 0.001$, and $p < 0.001$; Fig. 1E). The expression of α-SG in rAAV8-α-SG-injected TA muscle and surrounding muscles persisted more than 7 months (data not shown).

Expression of α-SG after injection of rAAV2-α-SG or rAAV8-α-SG into TA muscles of adult α-SG-deficient mice

Adult Sgca$^{-/-}$ mice (>4 weeks old) showed active cycles of the degeneration–regeneration process and had a mature immune system. To investigate whether injection of rAAV2-α-SG or rAAV8-α-SG could induce stable expression of α-SG in adult Sgca$^{-/-}$ skeletal muscle without cytotoxicity and immune response, we injected 5×10^{11} VG of rAAV2-α-SG or rAAV8-α-SG into the right TA muscles of adult Sgca$^{-/-}$ mice. Four weeks after rAAV2-α-SG injection, we did not observe α-SG-positive fibers in the right TA muscle (data not shown). rAAV2-α-SG-injected TA muscles showed the degeneration–regeneration process. In contrast, after rAAV8-α-SG injection, we observed numerous α-SG-positive fibers in the entirety of rAAV8-injected hind limb muscles (Fig. 2A). Moreover, α-SG-positive fibers were detected even in contralateral hind limb muscles and cardiac muscle (Fig. 2B and C). In particular, when rAAV8-α-SG was injected into the TA muscle of Sgca$^{+/+}$ mice, we observed no pathological changes in the injected hind limb muscles 4 weeks after injection (Fig. 2D). No signs of tissue damage were found in regions where α-SG was detected after injection of rAAV8-α-SG. α-SG-positive myofibers retained normal morphology up to 4 weeks after injection. In addition, to examine whether rAAV2-α-SG and rAAV8-α-SG administration affect liver function, we measured the serum level of liver-related isozymes including alanine aminotransferase (ALT), γ-glu-

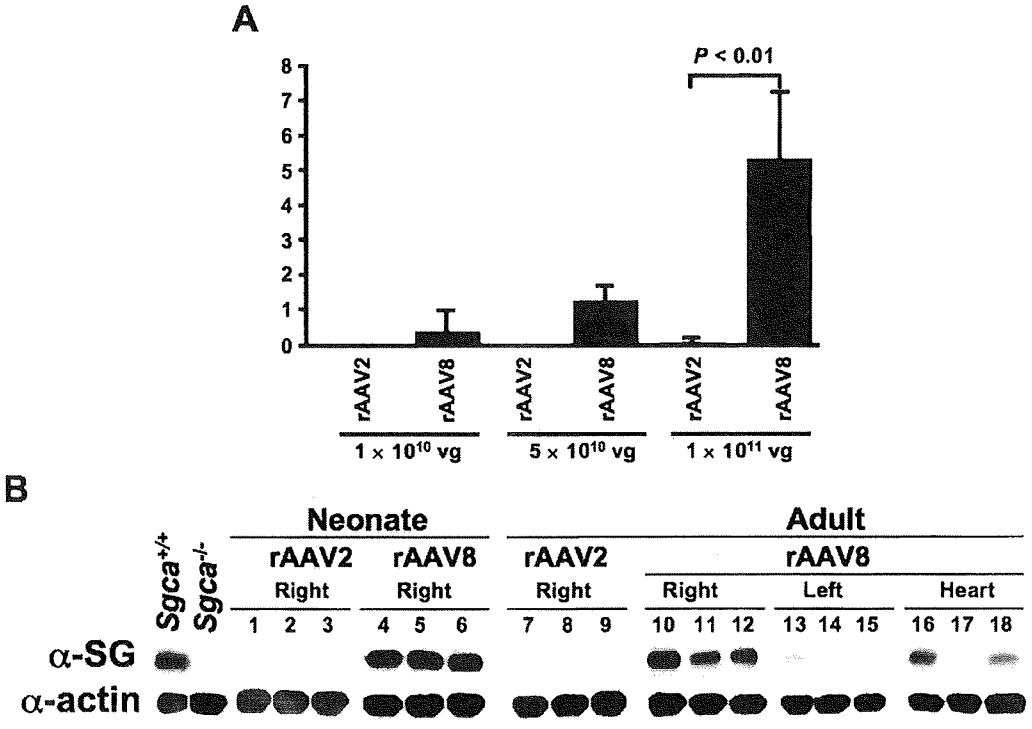

FIG. 3. Immunoblot analysis of α-SG in rAAV-injected α-SG-deficient muscles. Expression of α-SG in the hind limb muscles and heart of Sgca$^{-/-}$ mice was examined 4 weeks after rAAV injection, by real-time PCR and Western blot. (**A**) Real-time PCR was performed in duplicate to quantitate transgene copy number in each hind limb muscle after a single intramuscular administration of rAAV2-α-SG and rAAV8-α-SG. The right TA muscle of neonatal Sgca$^{-/-}$ mice was transduced with vector at 1×10^{10}, 5×10^{10}, and 1×10^{11} VG. Results are represented as vector copy number per diploid genome together with standard errors of mean. p Values are indicated and show a significant difference between rAAV2- and rAAV8-injected Sgca$^{-/-}$ mice ($p < 0.001$). (**B**) The right TA muscles of Sgca$^{-/-}$ mice were transduced with 1×10^{11} VG (neonates) or 5×10^{11} VG (adults) of rAAV2-α-SG (lanes 1–3 and 7–9) or rAAV8-α-SG (lanes 4–6 and 10–18). Ten-microgram samples of muscle lysates were separated by 10% SDS–PAGE. Faint bands were detected in the contralateral hind limb muscles of rAAV8-α-SG-injected mice. Adult Sgca$^{+/+}$ and Sgca$^{-/-}$ hind limb muscle lysates were used as positive and negative controls, respectively. The α-SG antibody detected a 50-kDa band. α-Sarcomeric actin is shown as a loading control.